CHAPTER II

II. RESULTS AND DISCUTION

This study belongs to the most important category of surface active materials, which named metallocationic surfactant. There are different types of the cationic surfactant, our study concerning only with quaternary ammonium bromide salt (QABr) and their complexes. These salts were prepared by the quaternization reaction of fatty alkyl bromide with tertiary amine then complexing with $SnCl_2\ 2H_2O$ and $CoCl_2\ 6H_2O$. This reaction occurred in polar solvent yielding the QABr and their complexes. These products are purified, recrystalized, and stored (kept) for 48 hours before analysis.

2.1. Micro elemental analysis:

The micro elemental analysis used to determine the percentage of the elements in the compound.

Table (1): The micro elemental analysis of the prepared metallosurfactants.

Complex		M	N	X	Y	Z	A	B
C %	Th.	57.25	56.66	52.79	52.18	52.48	45.37	44.9
	Exp.	56.75	56.25	52.4	51.8	52.1	45.2	44.5
H %	Th.	7.84	8.43	8	8.69	8.36	6	6.6
	Exp.	7.7	8.2	7.9	8.5	8.2	5.9	6.5
N %	Th.	2.38	2.36	2.68	2.6	2.66	4.8	4.7
	Exp.	2.2	2.1	2.5	2.4	2.5	4.6	4.5

As shown in Table (1), it is clear that the theoretical and the found values of microanalysis are very close, this means that these compounds are pure, and their working out was done by right method.

2.2. Structure confirmation of the prepared complexes:

2.2.1. Structure confirmation of complex (M):

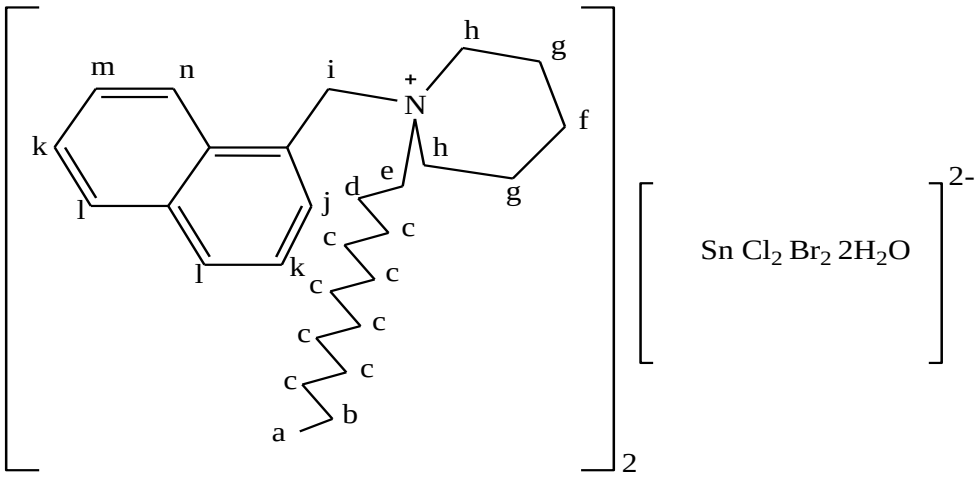

Fig. (7): Complex (M), N – methyl naphthalene – N – dodecyl pipyridinium dibromo – dichloro tinate complex.

The structure of complex (M), as shown in fig. (7), was confirmed using the following techniques:

i. Correct elemental analysis

ii. The IR spectrum showed absorption band at 778 cm^{-1} corresponding to adjacent H atom of naphthalene and absorption bands at 1450 cm^{-1} and 2847 cm^{-1} corresponding to CH aliphatic asymmetric bending and symmetric stretching respectively. It shows also absorption band at 2920 cm^{-1} corresponding to ammonium ion (R_4N^+), see fig. (14).

iii. ^{1}HNMR spectra showed signal triplet at δ= 0.87 ppm for (H_a), sextet at δ= 0.9 ppm for (H_b), quintet at δ= 1.29 ppm for (H_c), quintet at δ= 1.8 ppm for (H_d), triplet at δ= 3.07 ppm for (H_e), quintet at δ= 1.29 ppm for (H_f), quintet at δ= 2.56 ppm for (H_g),

triplet at δ= 3.44 ppm for (H_h), singlet at δ= 4.83 ppm for (H_i), doublet at δ= 7.1 ppm for (H_j), triplet at δ= 7.65 ppm for (H_k), doublet at δ= 7.93 ppm for (H_l), doublet at δ= 8.09 ppm for (H_m) and triplet at δ= 8.44 for (H_n), see fig. (21).

2.2.2. Structure confirmation of complex (N):

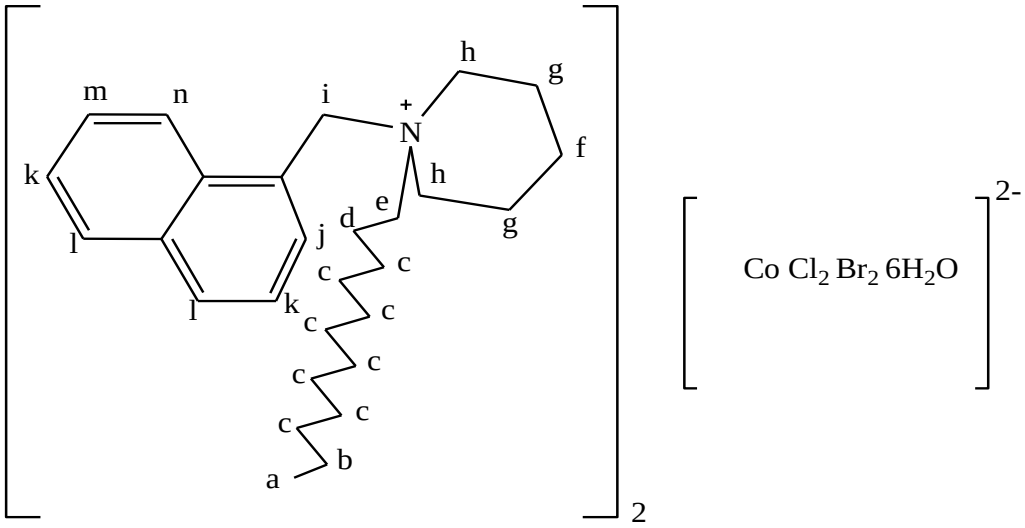

Fig. (8): Complex (N), N - methyl naphthalene – N - dodecyl pipyridinium dibromo – dichloro cobaltate complex.

The structure of complex (N) as shown in fig. (8) was confirmed using:

i. Correct elemental analysis.

ii. The IR spectrum showed absorption band at 722 cm^{-1} corresponding to adjacent H atoms of naphthalene and absorption bands at 1454 cm^{-1} and 2851 cm^{-1} corresponding to CH aliphatic asymmetric bending and symmetric stretching respectively. It shows also absorption band at 2920 cm^{-1} corresponding to ammonium ion (R_4N^+) and absorption band at 3408 cm^{-1} corresponding to OH group, see fig. (15).

iii. ^{1}HNMR spectra showed signal triplet at δ= 0.85 ppm for (H_a), sextet at δ= 0.8 ppm for (H_b), quintet at δ= 1.25 ppm for (H_c), quintet at δ= 1.66 ppm for (H_d), triplet at δ= 2.97 ppm for (H_e), quintet at δ= 1.25 ppm for (H_f), quintet at δ= 2.56 ppm for (H_g), triplet at δ= 3.6 ppm for (H_h), singlet at δ= 4.88 ppm for (H_i), doublet at δ= 7.07 ppm for (H_j), triplet at δ= 7.56 ppm for (H_k), doublet at δ= 7.71 ppm for (H_l), doublet at δ= 7.96 ppm for (H_m) and triplet at δ= 8.3 for (H_n), see fig. (22).

2.2.3. Structure confirmation of complex (X):

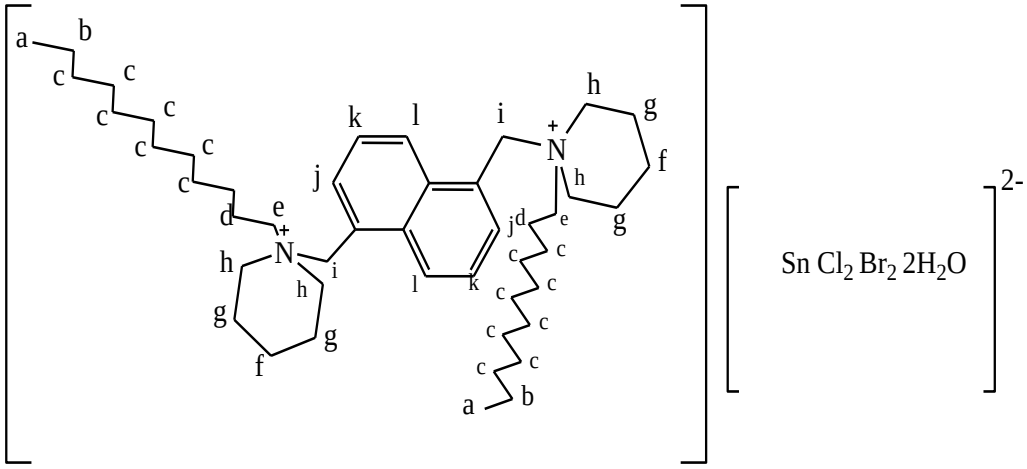

Fig. (9): Complex (X), N, N' -1, 5 Bis dimethyl naphthalene – N, N' - didodecyl dipipyridinium dibromo – dichloro tinate complex.

The structure of complex (X) as shown in fig. (9) was confirmed using:

i. Correct elemental analysis.

ii. The IR spectrum showed absorption band at 784 cm^{-1} corresponding to adjacent H atoms of naphthalene and absorption bands at 1455 cm^{-1} and 2851 cm^{-1} corresponding to

CH aliphatic asymmetric bending and symmetric stretching respectively. It shows also absorption band at 2922 cm^{-1} corresponding to ammonium ion (R_4N^+) and absorption band at 3452 cm^{-1} corresponding to OH group, see fig. (16).

iii. ^{1}HNMR spectra showed signal triplet at δ= 0.87 ppm for (H_a), sextet at δ= 1.13 ppm for (H_b), quintet at δ= 1.29 ppm for (H_c), quintet at δ= 1.7 ppm for (H_d), triplet at δ= 3.07 ppm for (H_e), quintet at δ= 1.29 ppm for (H_f), quintet at δ= 2.56 ppm for (H_g), triplet at δ= 3.4 ppm for (H_h), singlet at δ= 4.83 ppm for (H_i), doublet at δ= 7.14 ppm for (H_j), triplet at δ= 7.61 ppm for (H_k) and doublet at δ= 7.68 ppm for (H_l), see fig. (23).

2.2.4. Structure confirmation of complex (Y):

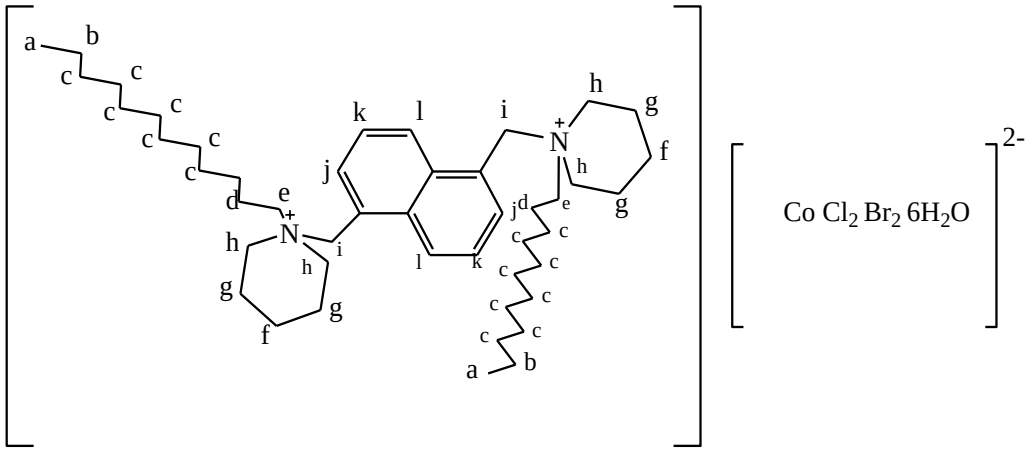

Fig. (10): Complex (Y), N, N' -1, 5 Bis dimethyl naphthalene – N, N' – didodecyl dipipyridinium dibromo – dichloro cobaltate complex.

The structure of complex (Y) as shown in fig. (10) was confirmed using:

i. Correct elemental analysis.

ii. The IR spectrum showed absorption band at 786 cm^{-1} corresponding to adjacent H atoms of naphthalene and absorption bands at 1455 cm^{-1} and 2851 cm^{-1} corresponding to CH aliphatic asymmetric bending and symmetric stretching respectively. It shows also absorption band at 2922 cm^{-1} corresponding to ammonium ion (R_4N^+) and absorption band at 3427 cm^{-1} corresponding to OH group, see fig. (17).

iii. ^{1}HNMR spectra showed signal triplet at δ= 0.84 ppm for (H_a), sextet at δ= 1.1 ppm for (H_b), quintet at δ= 1.24 ppm for (H_c), quintet at δ= 1.66 ppm for (H_d), triplet at δ= 2.99 ppm for (H_e), quintet at δ= 1.24 ppm for (H_f), quintet at δ= 2.56 ppm for (H_g), triplet at δ= 3.8 ppm for (H_h), singlet at δ= 4.61 ppm for (H_i), doublet at δ= 7.59 ppm for (H_j), triplet at δ= 7.78 ppm for (H_k) and doublet at δ= 7.97 ppm for (H_l), see fig. (24).

2.2.5. Structure confirmation of complex (Z):

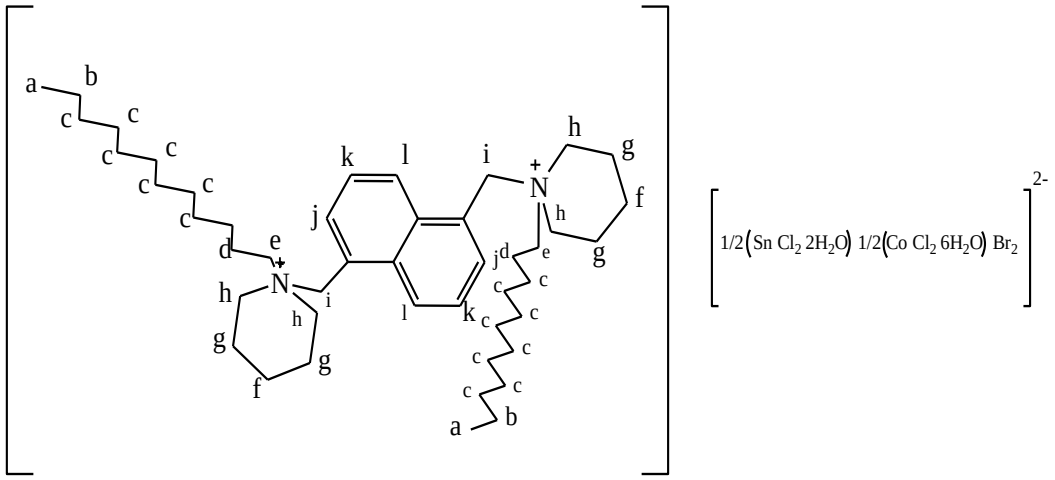

Fig. (11): Complex (Z), N, N' -1, 5 Bis dimethyl naphthalene – N, N' – didodecyl dipipyridinium dibromo – dichloro tinate cobaltate complex.

The structure of complex (Z) as shown in fig. (11) was confirmed using:

i. Correct elemental analysis.

ii. The IR spectrum showed absorption band at 720 cm^{-1} corresponding to adjacent H atoms of naphthalene and absorption bands at 1455 cm^{-1} and 2851 cm^{-1} corresponding to CH aliphatic asymmetric bending and symmetric stretching respectively. It shows also absorption band at 2922 cm^{-1} corresponding to ammonium ion (R_4N^+) and absorption band at 3398 cm^{-1} corresponding to OH group, see fig. (18).

iii. ^{1}HNMR spectra showed signal triplet at δ= 0.85 ppm for (H_a), sextet at δ= 1.1 ppm for (H_b), quintet at δ= 1.24 ppm for (H_c), quintet at δ= 1.7 ppm for (H_d), triplet at δ= 3 ppm for (H_e), quintet at δ= 1.24 ppm for (H_f), quintet at δ= 2.56 ppm for (H_g),

triplet at δ= 3.79 ppm for (H_h), singlet at δ= 4.7 ppm for (H_i), doublet at δ= 7.61 ppm for (H_j), triplet at δ= 7.85 ppm for (H_k) and doublet at δ= 8.02 ppm for (H_l), see fig. (25).

2.2.6. Structure confirmation of complex (A):

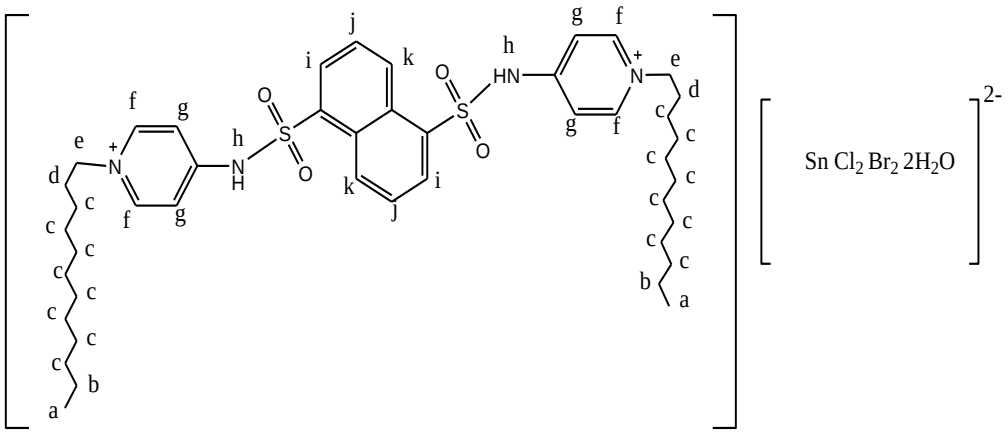

Fig. (12): Complex (A), 4, 4' -1, 5 Bis disulfonamide naphthalene – N, N' – didodecyl dipyridinium dibromo – dichloro tinate complex.

The structure of complex (A) as shown in fig. (12) was confirmed using:

i. Correct elemental analysis.

ii. The IR spectrum showed absorption band at 758 cm^{-1} corresponding to adjacent H atoms of naphthalene and absorption band at 1189 cm^{-1} corresponding to SO_2-NH group. It shows also absorption band at 2927 cm^{-1} corresponding to ammonium ion (R_4N^+) and absorption band at 3428 cm^{-1} corresponding to OH group, see fig. (19).

iii. ^{1}HNMR spectra showed signal triplet at δ= 0.85 ppm for (H_a), sextet at δ= 1.24 ppm for (H_b), quintet at δ= 1.53 ppm for (H_c), quintet at δ= 1.49 ppm for (H_d), triplet at δ= 2.53 ppm for (H_e),

doublet at δ= 8.9 ppm for (H_f), doublet at δ= 6.8 ppm for (H_g), singlet at δ= 4.6 ppm for (H_h), doublet at δ= 8.1 ppm for (H_i), triplet at δ= 7.4 ppm for (H_j) and doublet at δ= 7.5 ppm for (H_k), see fig. (26).

2.2.7. Structure confirmation of complex (B):

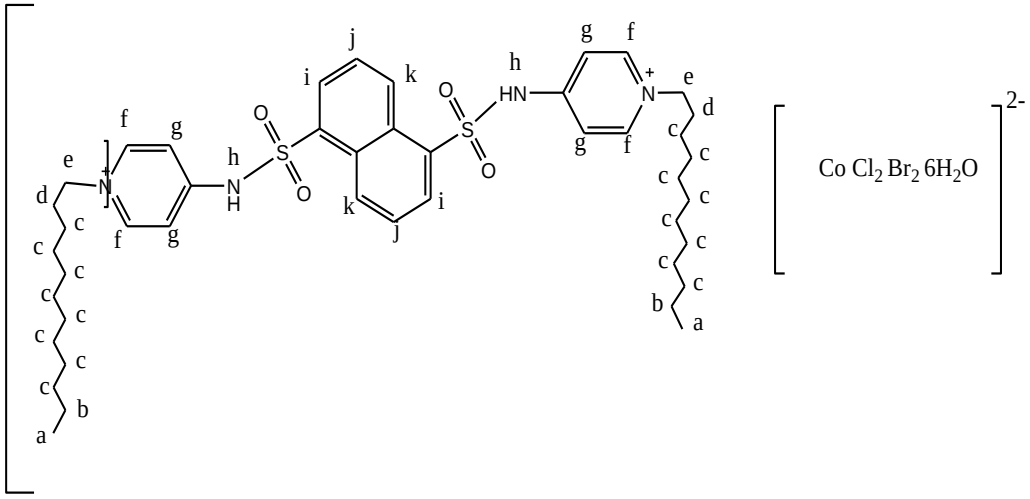

Fig. (13): Complex (B), 4, 4' - 1, 5 Bis disulfonamide naphthalene – N, N' didodecyl dipyridinium dibromo – dichloro cobaltate complex.

The structure of complex (B) as shown in fig. (13) was confirmed using:

i. Correct elemental analysis.

ii. The IR spectrum showed absorption band at 762 cm^{-1} corresponding to adjacent H atoms of naphthalene and absorption band at 1190 cm^{-1} corresponding to SO_2-NH group. It shows also absorption band at 2971 cm^{-1} corresponding to

ammonium ion (R_4N^+) and absorption band at 3395 cm^{-1} corresponding to OH group, see fig. (20).

iii. ^{1}HNMR spectra showed signal triplet at δ= 0.96 ppm for (H_a), sextet at δ= 1.15 ppm for (H_b), quintet at δ= 1.41 ppm for (H_c), quintet at δ= 1.4 ppm for (H_d), triplet at δ= 2.56 ppm for (H_e), doublet at δ= 8.9 ppm for (H_f), doublet at δ= 6.7 ppm for (H_g), singlet at δ= 4.5 ppm for (H_h), doublet at δ= 7.96 ppm for (H_i), triplet at δ= 7.3 ppm for (H_j) and doublet at δ= 7.38 ppm for (H_k), see fig. (27).

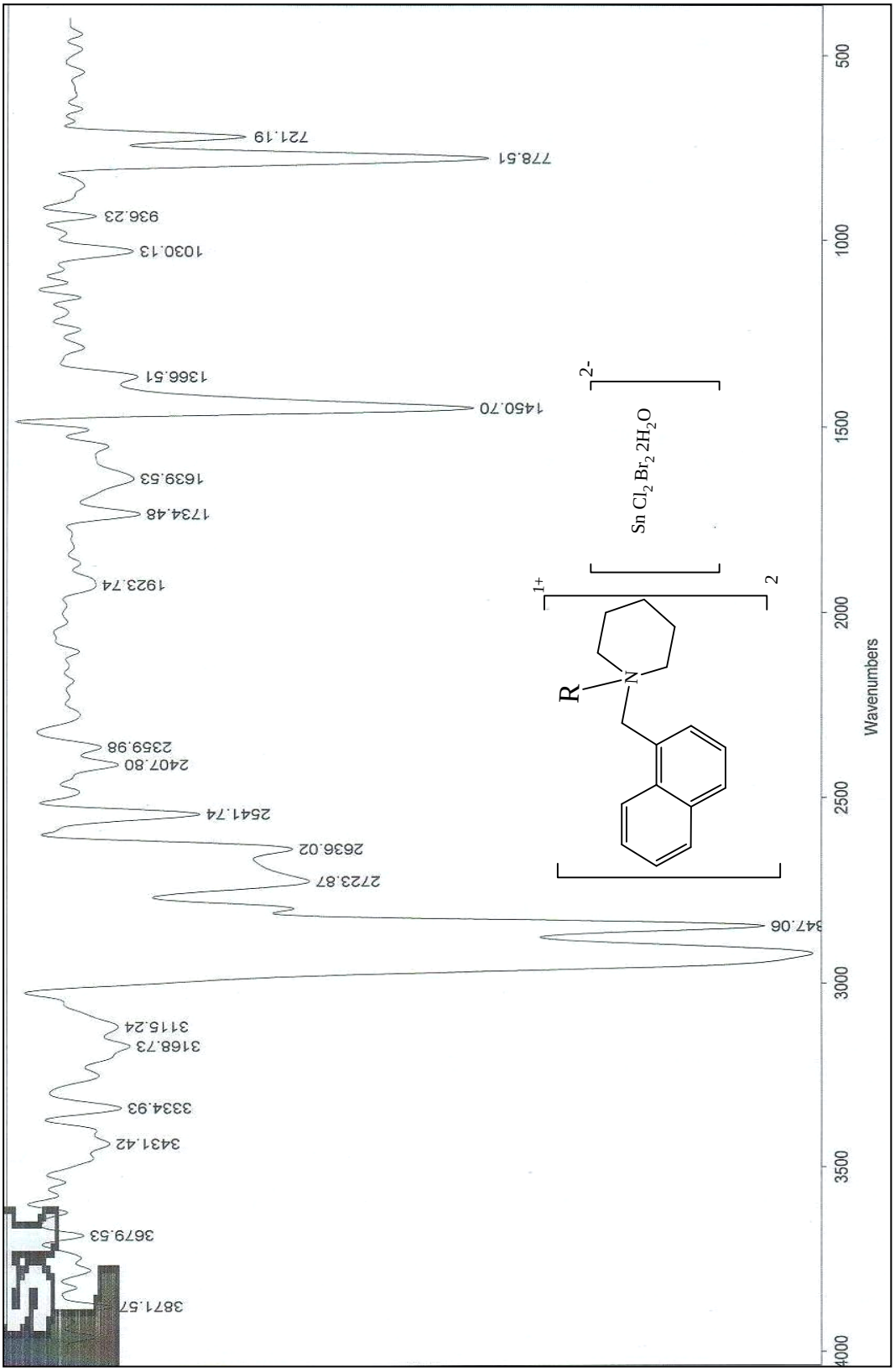

Fig. (14): FTIR - Spectrum of the metallocationic surfactant (M).

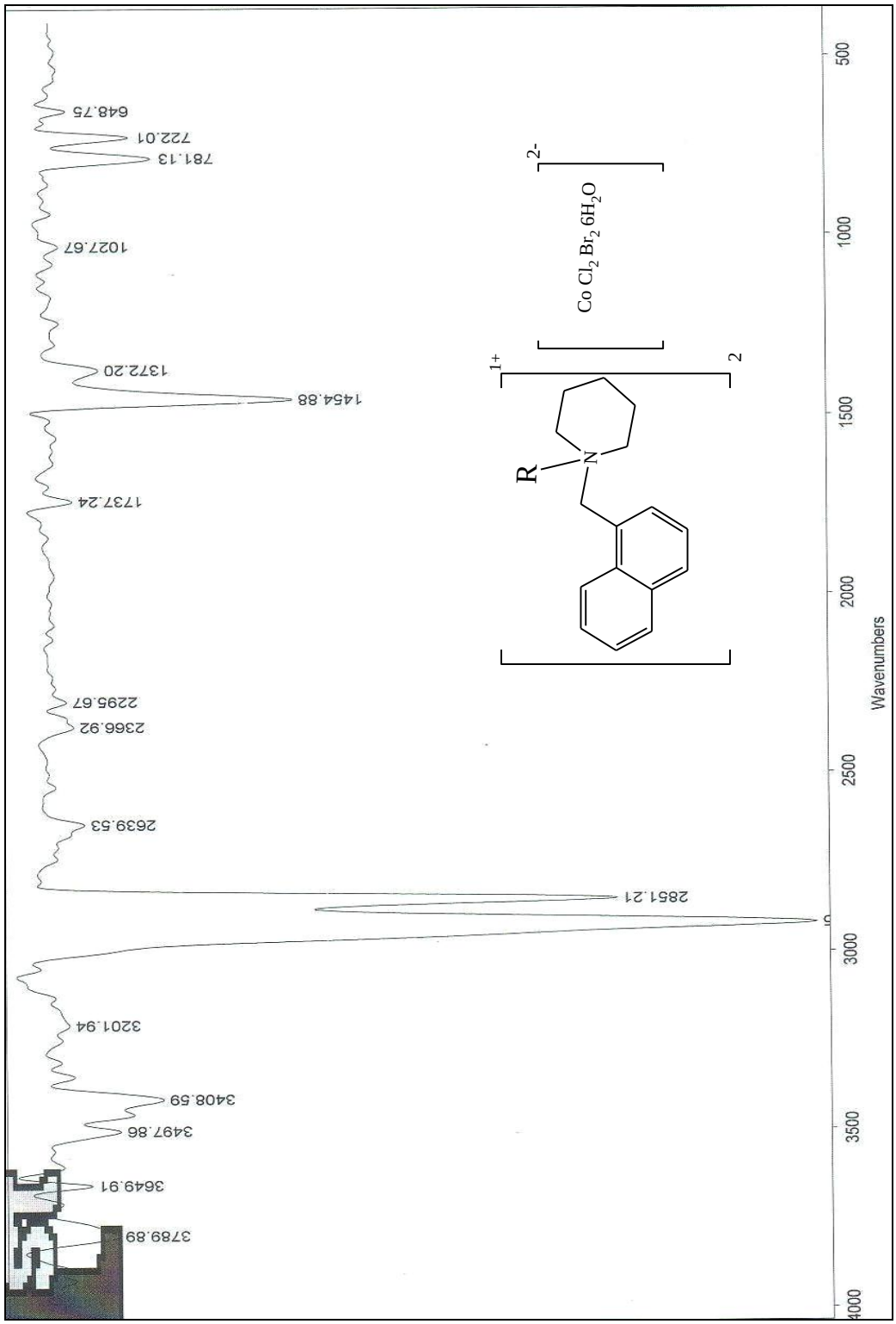

Fig. (15): FTIR - Spectrum of the metallocationic surfactant (N).

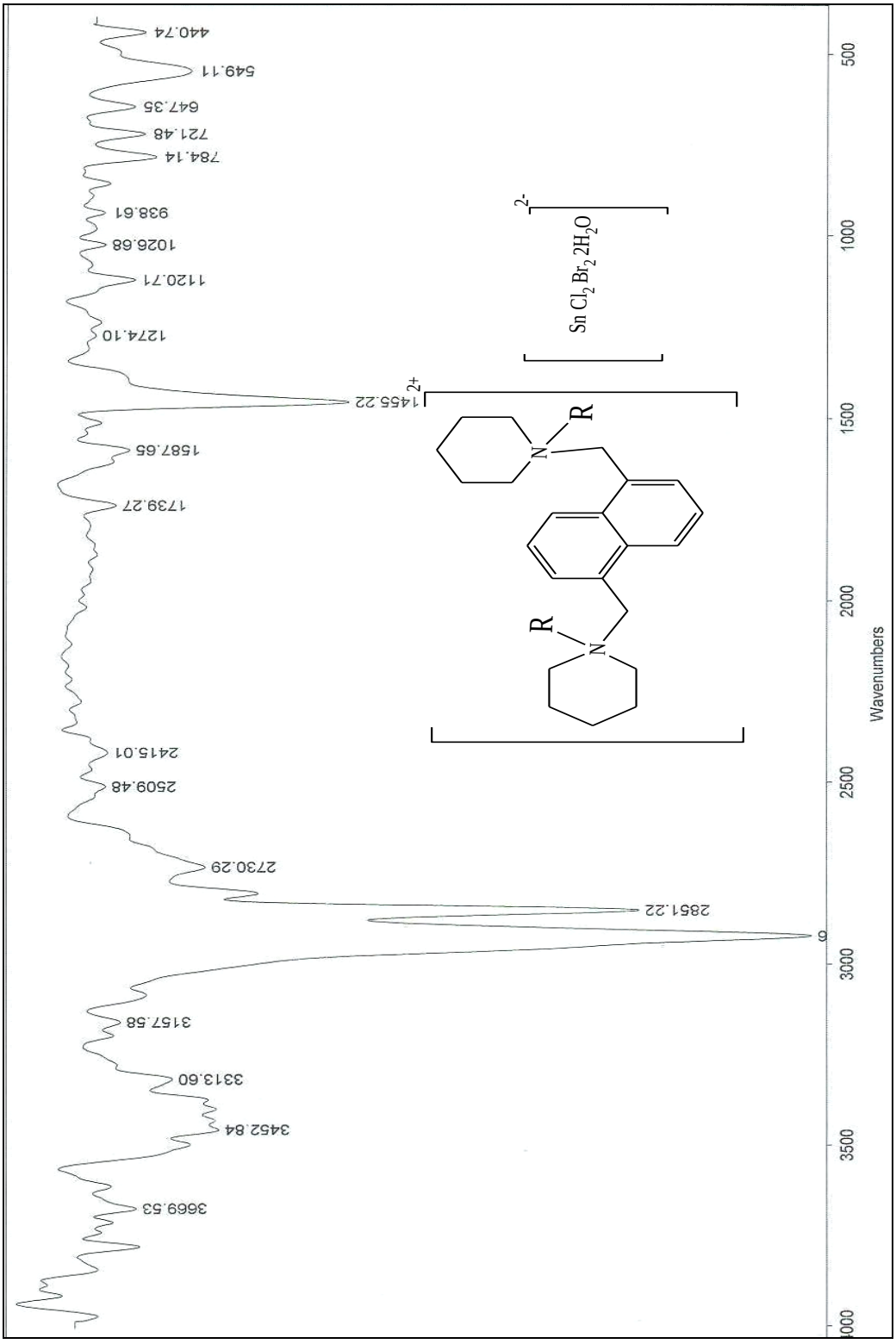

Fig. (16): FTIR - Spectrum of the metallocationic surfactant (X).

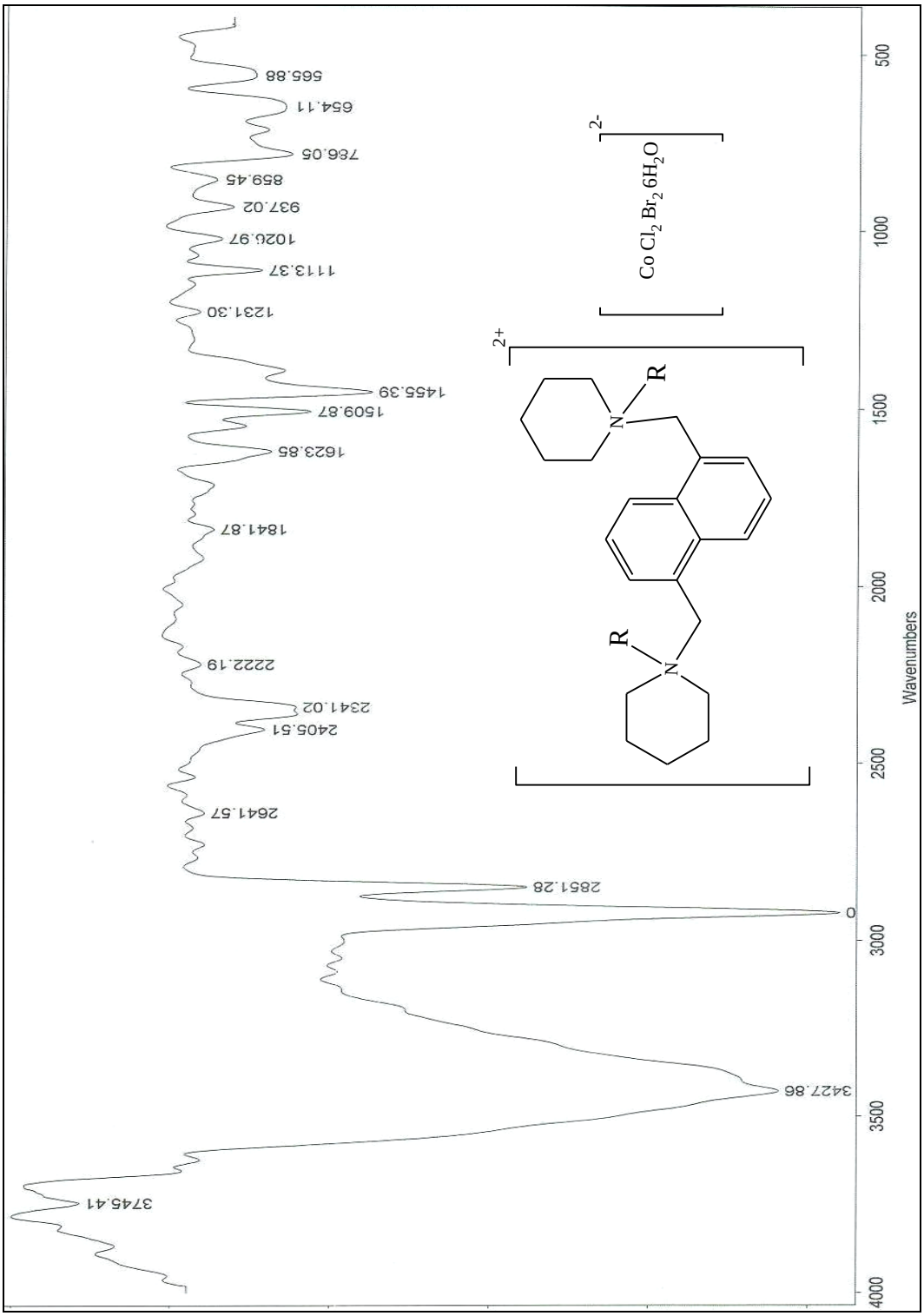

Fig. (17): FTIR - Spectrum of the metallocationic surfactant (Y).

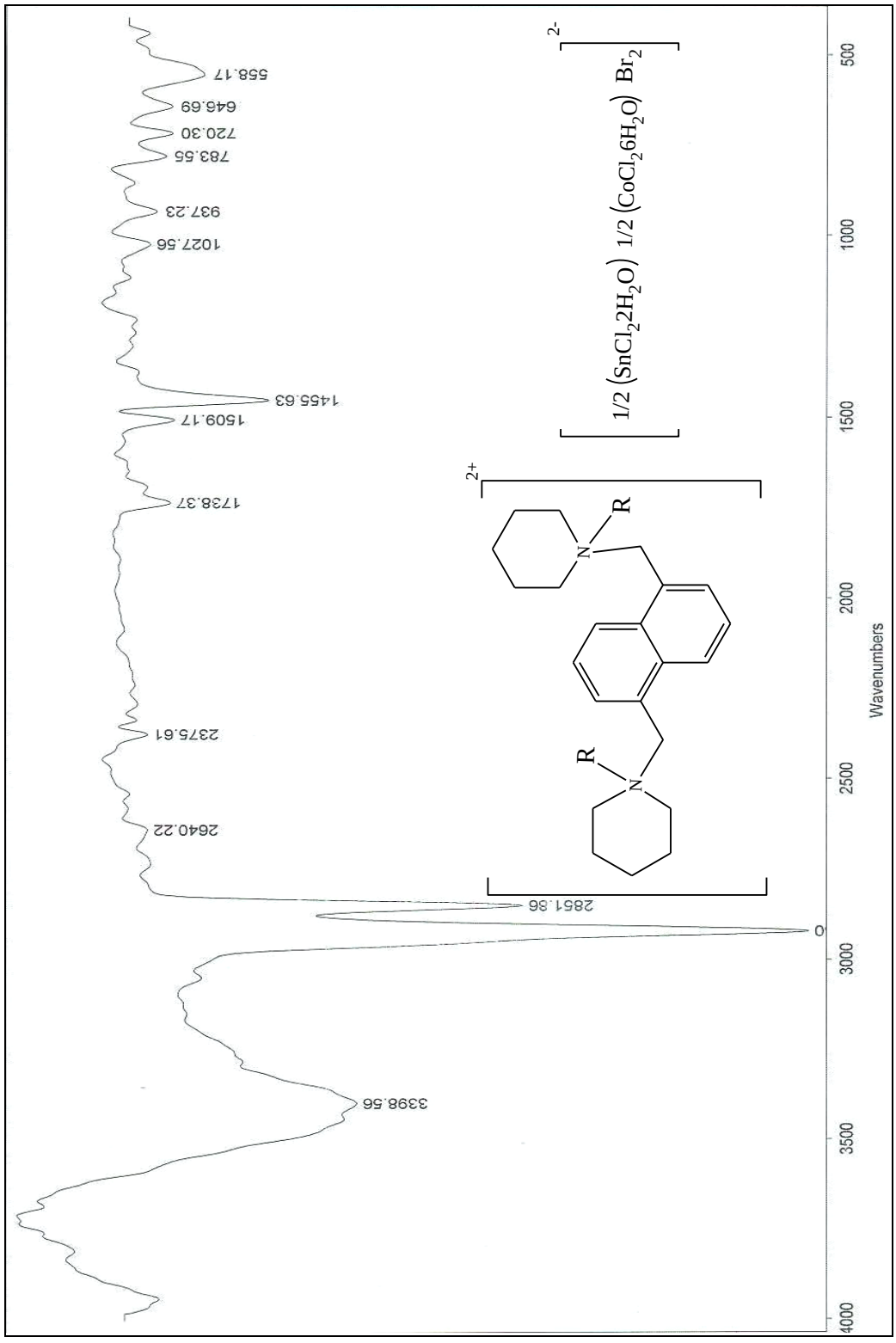

Fig. (18): FTIR - Spectrum of the metallocationic surfactant (Z).

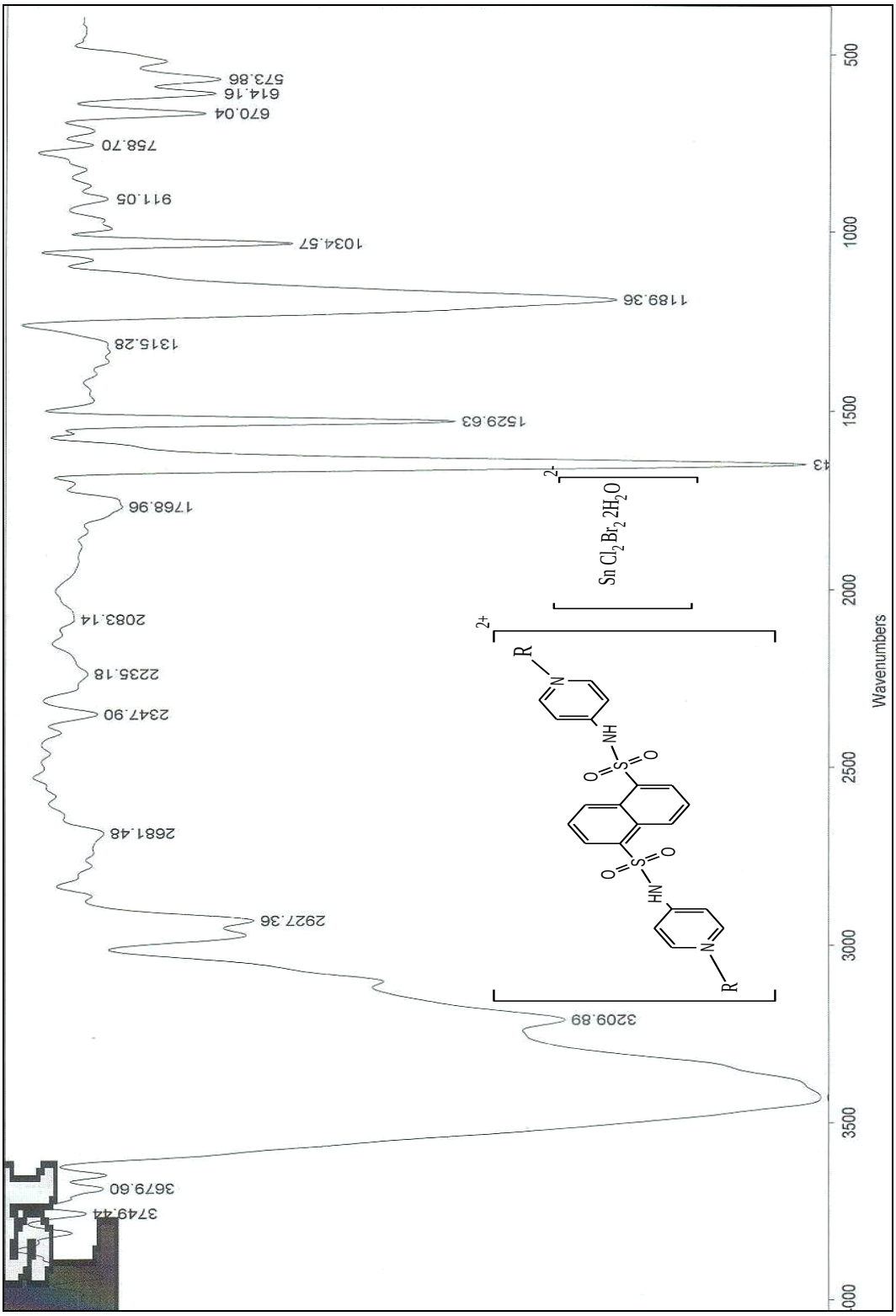

Fig. (19): FTIR - Spectrum of the metallocationic surfactant (A)

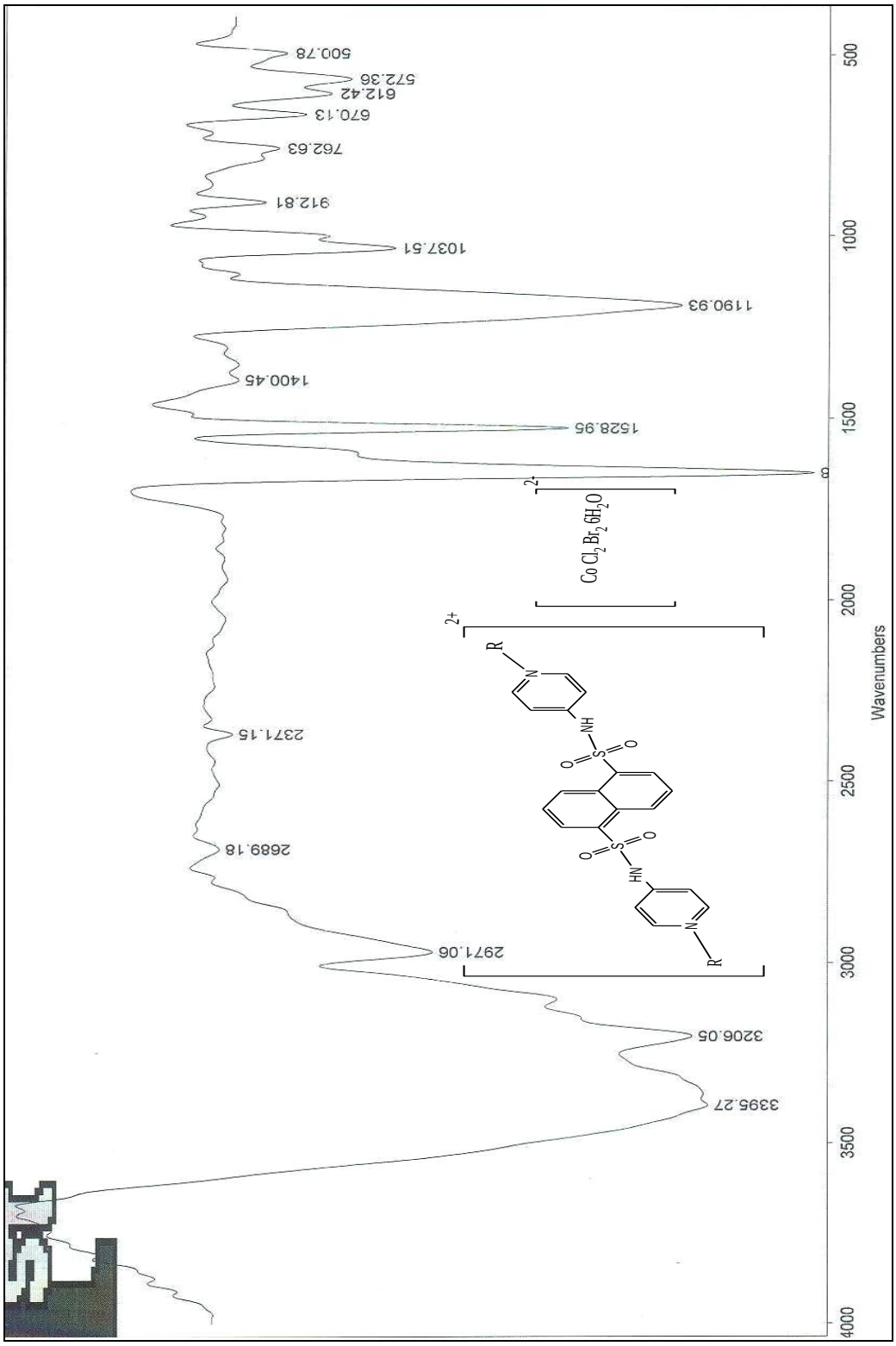

Fig. (20): FTIR - Spectrum of the metallocationic surfactant (B)

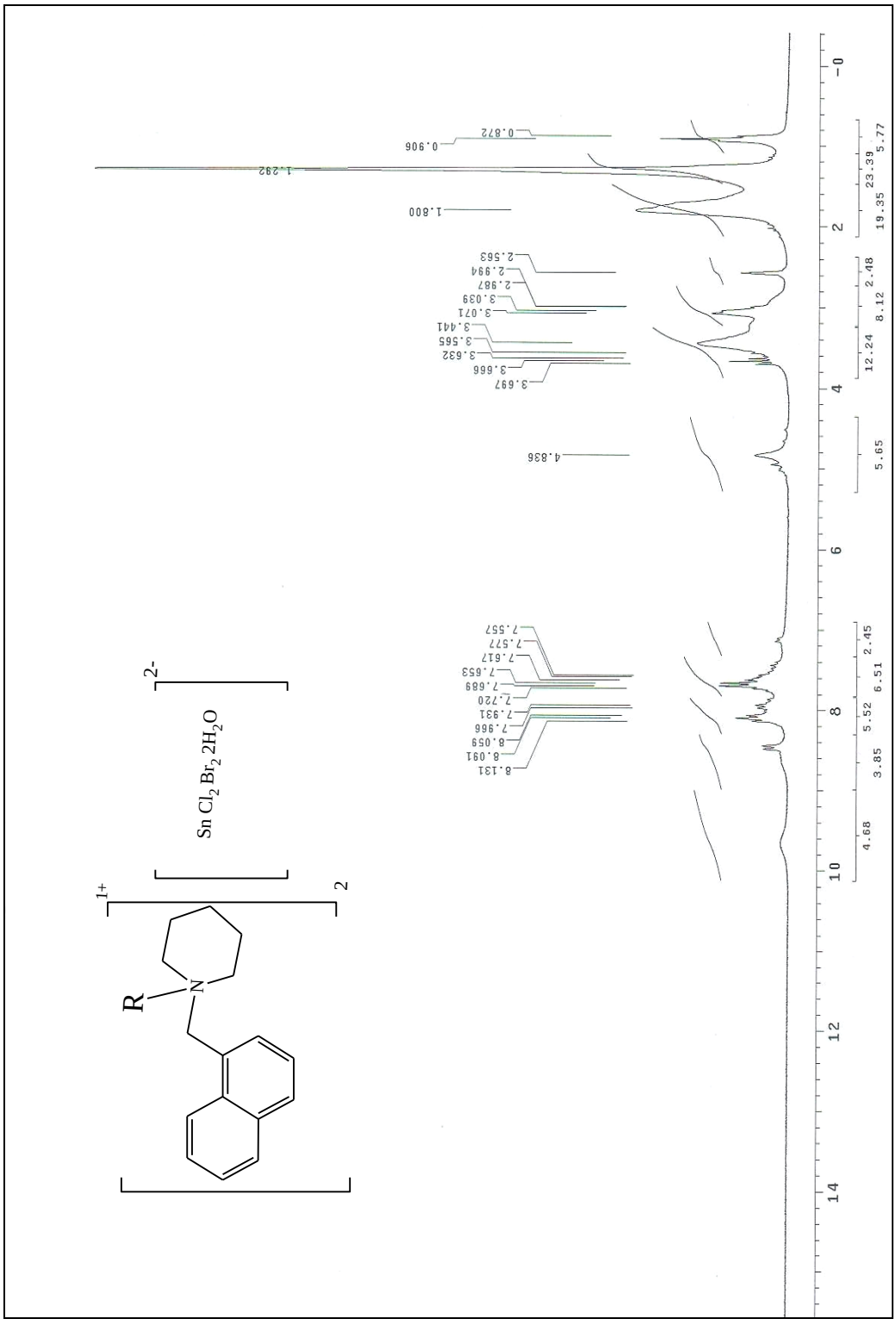

Fig. (21): ^{1}H-NMR - Spectrum of the metallocationic surfactant (M).

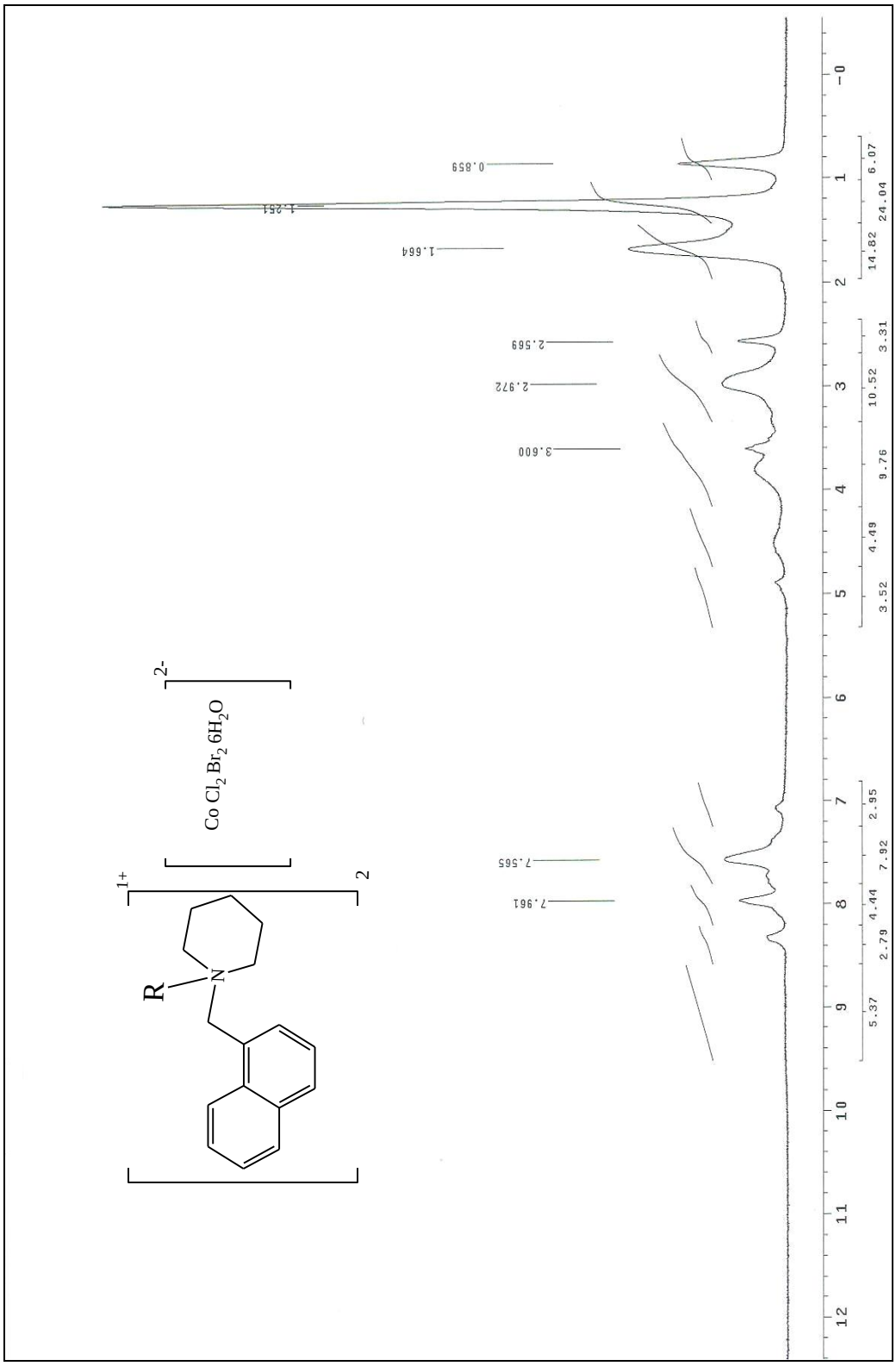

Fig. (22): ^{1}H-NMR - Spectrum of the metallocationic surfactant (N).

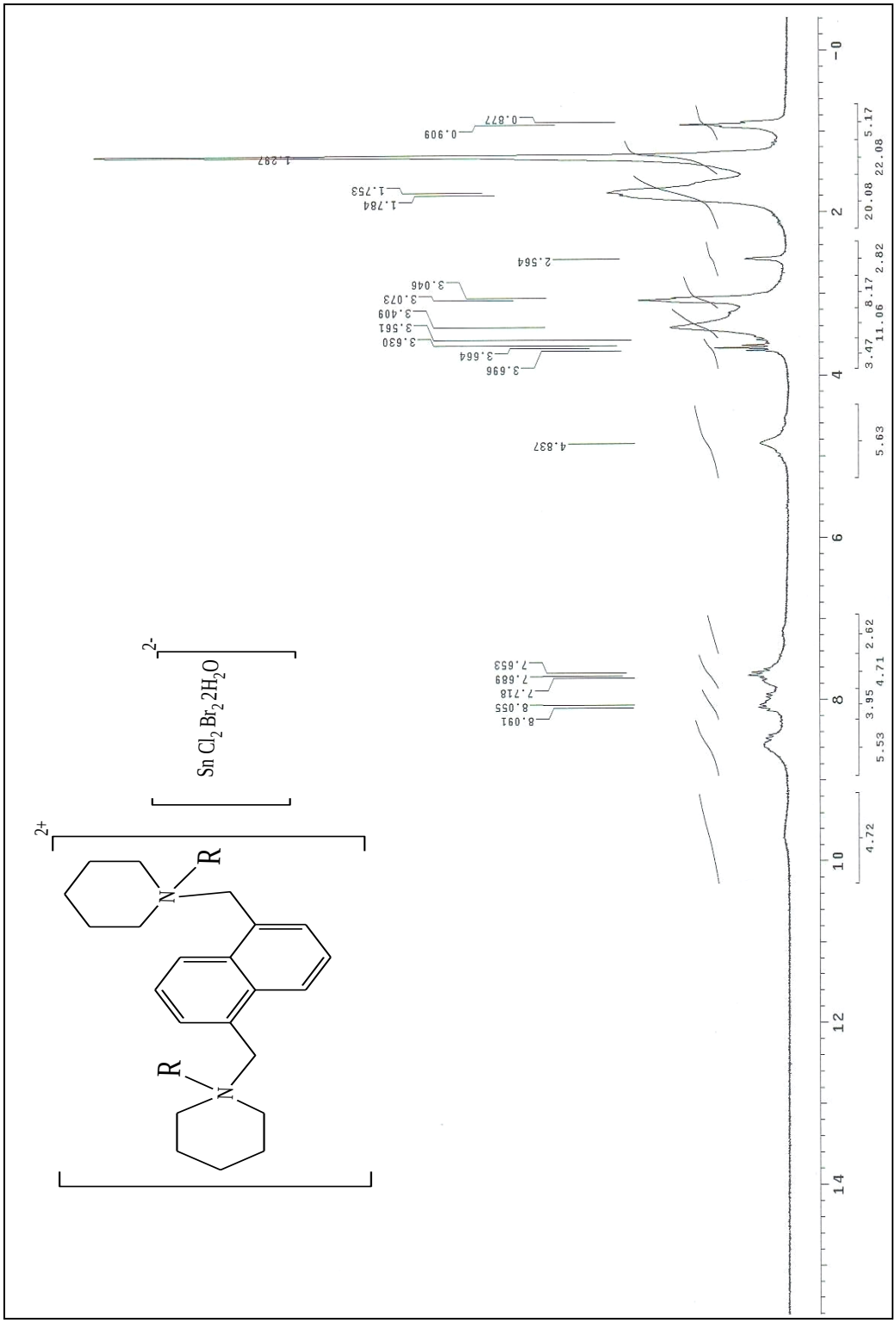

Fig. (23): ^{1}H-NMR - Spectrum of the metallocationic surfactant (X).

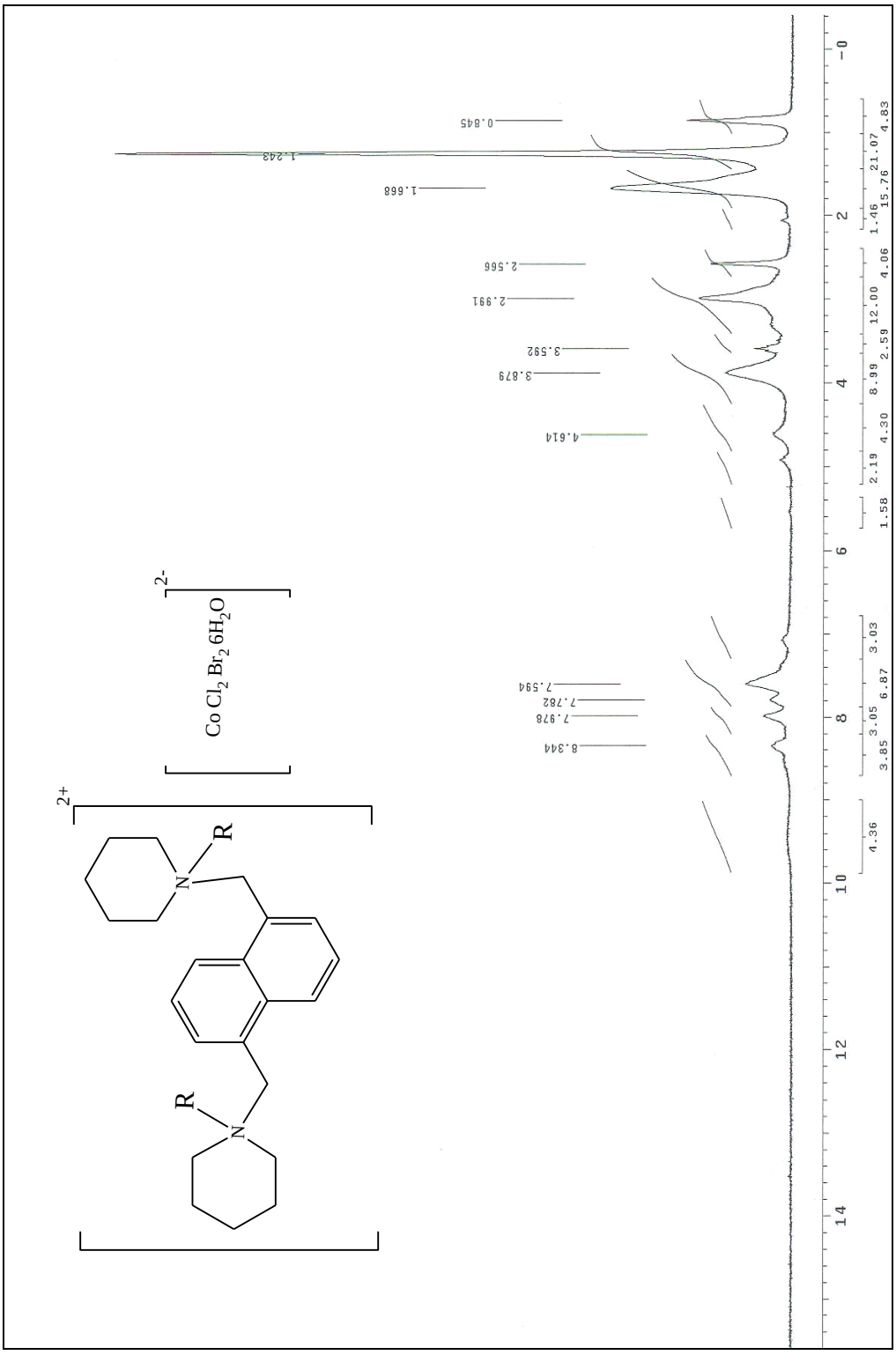

Fig. (24): ^{1}H-NMR - Spectrum of the metallocationic surfactant (Y).

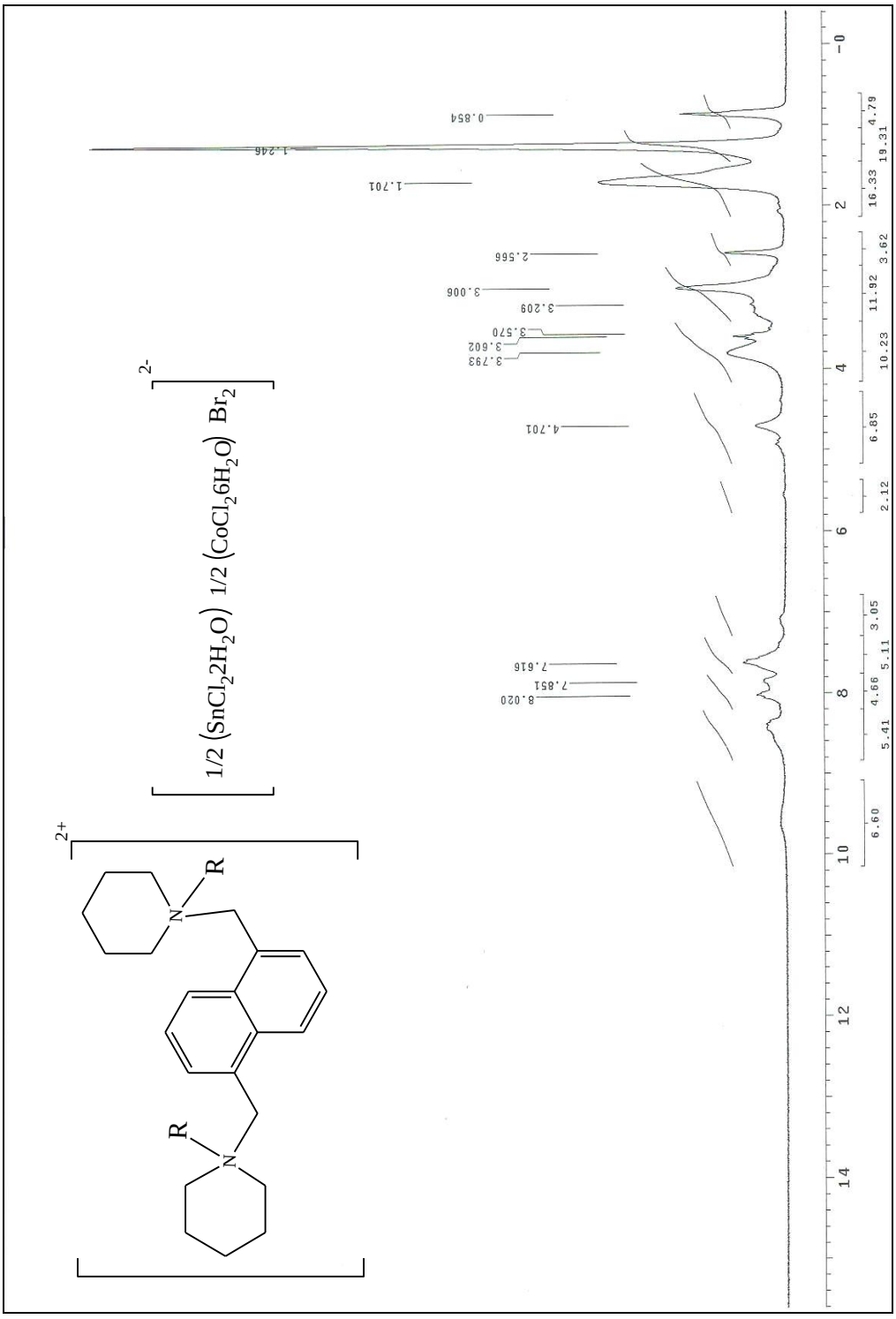

Fig. (25): ^{1}H-NMR - Spectrum of the metallocationic surfactant (Z).

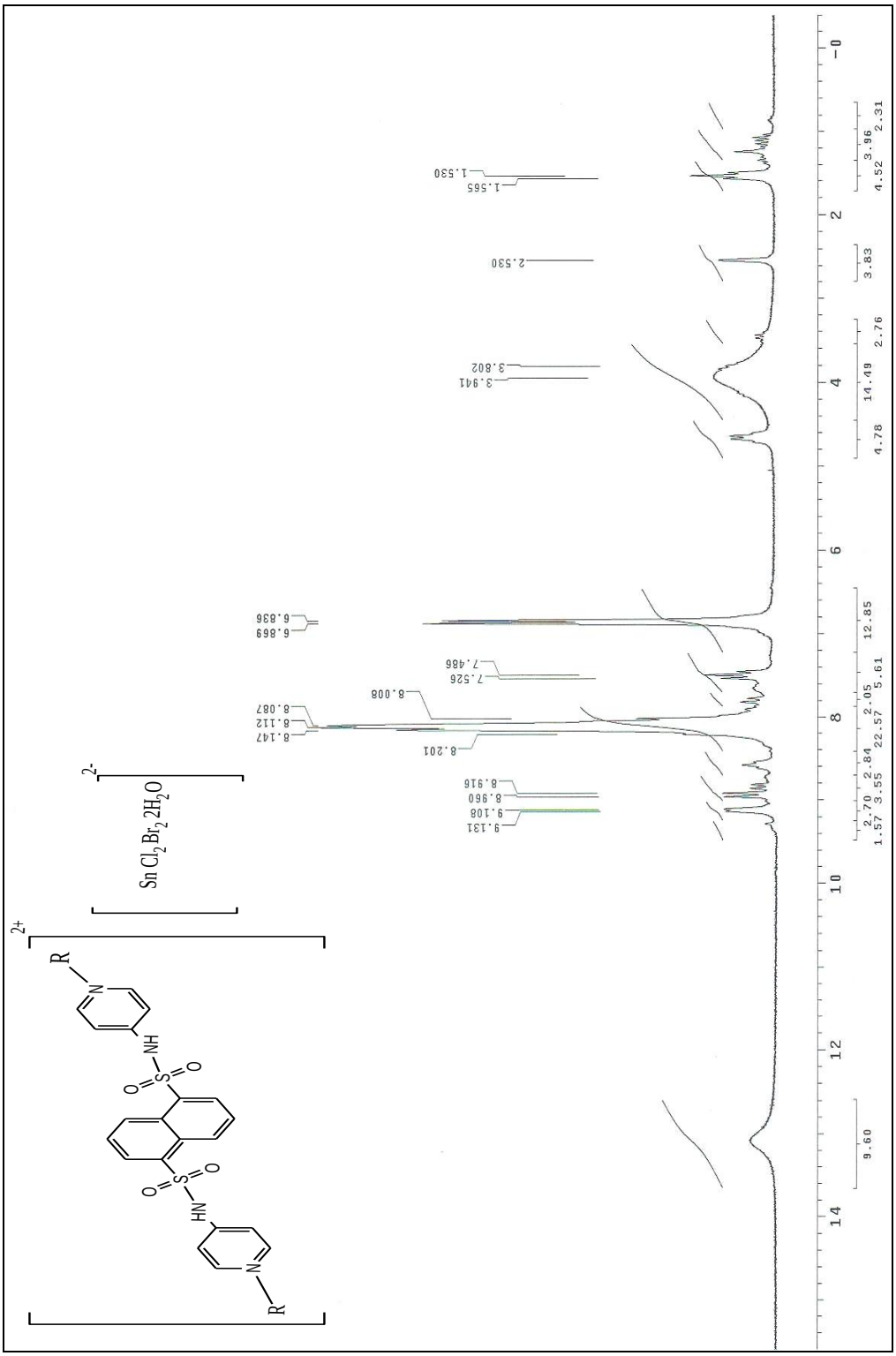

Fig. (26): ^{1}H-NMR - Spectrum of the metallocationic surfactant (A).

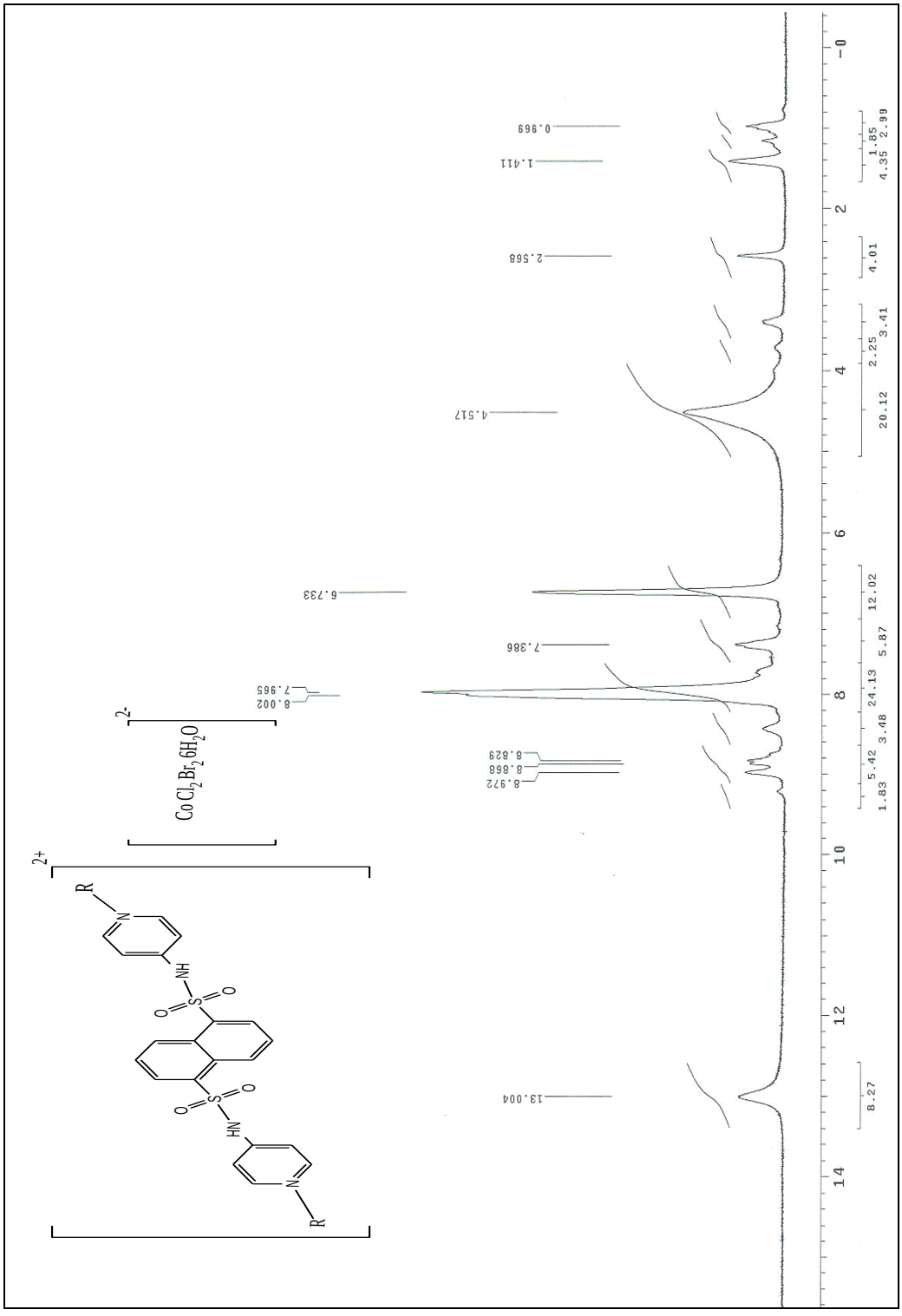

Fig. (27): ^{1}H-NMR - Spectrum of the metallocationic surfactant (B).

2.3. Surface properties of the prepared metallosurfactant compounds:

The influence of the structure and the molecular weight of the prepared metallosurfactants on the physical properties were assessed. Surface properties such as surface tension, interfacial tension and emulsifying power of these metallosurfactants were investigated. The surface parameters including Critical micelle concentration (CMC), Efficiency (Pc_{20}), Effectiveness (π_{CMC}), maximum surface excess (Γ_{max}) and minimum surface area (A_{min}) were studied. Free energy of micellization (ΔG^{o}_{mic}) and adsorption (ΔG^{o}_{ads}) were calculated. Tables (11-19) list these properties.

2.3.1. Surface and interfacial tension:

Surface tension is a characteristic property for the liquids and it attributed to the attraction forces between the molecules at the surface. The surface tension value of the distilled water at (25 ^{o}C) was found (72 dyne/cm), which is attributed to the attraction forces between water molecules at the water surface due to the hydrogen bonds. If any foreign molecules present at the water surface leads to disturb that tension and decrease it. Meanwhile, surfactant molecules tend to be adsorbed at the air-water interface at lower concentrations due to the hydrophobic part (non polar phase) which decrease the aqueous solubility due to the repulsion occurred between it and the water molecules (polar phase) and the surfactant molecules forced to migrate from the bulk of the solution to the interface to reduce that repulsion.

Hence, by increasing the surfactant concentration, the surface tension of the resulted solution decreases gradually.

Surfactant metal complexes (metallosurfactants) are expected to provide a wide range of interesting phenomena on aggregation in aqueous solutions due to variations in charge numbers, size and extent of hydrophobicity through combination of the central metal and ligands[82]. However, their physical properties in solutions have not been extensively studied[83-87]. In previous studies, novel characteristics of surfactant metal complexes have been revealed and the results should provide significant information on surfactant solution chemistry. Metalloaggregates are made of surfactants that combine a metal-coordinating polar head to hydrophobic tail[88]. The polar head of the surfactant is functionalized with metal ions bound to and surrounded by a hydrophobic region, similar to the situation found in metalloproteinase[89].

The surface tension was measured at different concentrations (0.05, 0.025, 0.01, 0.005, 0.0025, 0.00125 and 0.001 mole/liter) and at different temperatures 25, 35 and 45 ^{o}C.

The surface tension values of the synthesized cationic surfactant II_c was plotted against (– log concentration) at 35 ^{o}C in fig. (28). While the surface tension values of the synthesized metallosurfactants were plotted against (– log concentration) at different temperatures (25, 35 and 45 ^{o}C) in figs. (29-35).

The figures showed that there are two characteristic regions. The first region at lower concentrations, in it the surface tension is greatly

sensitive towards concentration variations. The second region at higher concentrations, in it the surface tension is almost constant upon variation of surfactant concentration.

The intersection between the two regions determines the critical micelle concentration (CMC).

At lower concentrations, the surface tension values of the metallosurfactant solutions are high. Increasing the surfactant concentration leads to decrease the surface tension. This decrease can be referred to the accumulation of the surfactant molecules at the interface which disturb the binding forces between water molecules leading to decrease the surface tension to considerable values.

Also the figures showed that the surface tension values decrease as the temperature increase from 25 to 45 ^{o}C and this is because the surfactants become less soluble due to dehydration of the hydrophobic chain as the temperature increases. This is opposed by hydration of the hydrophilic group (increased monomer solubility arising from kinetic thermal effects with increasing temperature). The CMC values show a decreasing trend as the temperature increases.

The synthesized surfactants showed a great decrease in the surface tension values by increasing the concentrations. This decrease in the surface tension depends mainly on the hydrophobic chain length and the number of it in each compound of these surfactants and also the presence of the metal ion.

These results explain that the complexes retain its unity of structure in their solutions, which increased their volume in the aqueous media

with repulsion between the hydrophobic chains and the water molecules.

This repulsion facilitates two processes at the same time. The adsorption process of the molecules of metal complexes at the air/water interface of extremely lower concentrations (below CMC) and the micellization process of these molecules at concentrations lower than their parent salts.[90]

It is expected that the surface tension values of the cationic complexes (M, N, X, Y, Z, A and B) have lower values than the parent cationic surfactants (I_c, II_c and III_c). That could be due to the increase in the hydrophobicity of these complexes in comparison to the parent cationics, which is due to the presence of two ligands coordinated to the metal ion like (M and N) complexes, i.e., more non-polar chains. Then the water/surfactant molecules interactions increase, which forced them to the air-water interface[91]. Hence, the surface tension was depressed considerably.

Also, the presence of two alkyl chains in one molecule linked by a metal ion like (X, Y, Z, A and B) complexes, enhance the adsorption and the aggregation properties, by strengthening the inter- or intra-molecular hydrophobic interaction[92]. i.e., the complexes have more efficiency towards adsorption at air/water interface than their parent salts.

So, the structures of the synthesized surfactants play an important role in their surface properties.

The higher number of uniqueness of the metal-surfactant coordination complexes lies in the face that the bond between the head group and the tail part of the surfactant is a coordinate bond and the surfactant contains a higher charge on the head group which leads to more repulsion in the bulk of the aqueous solution and increasing adsorption on to the surface.

The interfacial tension of the oil/surfactant systems at (25 ^{o}C) was measured and the data was listed in table (2). It is clear from the data that the synthesized surfactants (M, N, X, Y, Z, A and B) have good interfacial tension values against paraffin oil. Also, the lower values of the interfacial tension indicate the ability of using these surfactants in several applications as corrosion inhibitor and biocides.

2.3.2. Emulsion stability:

The emulsifying power of the prepared cationic surfactants M, N, X, Y, Z, A and B are listed in table (2) as a function of time. It is clear that the emulsifying power depends commonly on the length and nature of the alkyl groups of the surfactant used. As shown in the table (2), the all prepared cationic surfactants have in general low emulsion stability as a function of time, so that these surfactants can not be used as long term emulsion stabilizers.

Table (2): Interfacial tension and emulsion stability of the synthesized metallosurfactants.

Compounds	Interfacial Tension, dyne/cm	Emulsion stability, Sec.
M	4	20
N	5	18
X	5	21
Y	3	19
Z	5	25
A	3	142
B	5	85

Table (3): Surface tension at different concentrations of sample (II_c) at 35 ºC.

- log C	1.3	1.6	2	2.3	2.6	2.9	3
35 °C	32	34	36	39	43	48	52

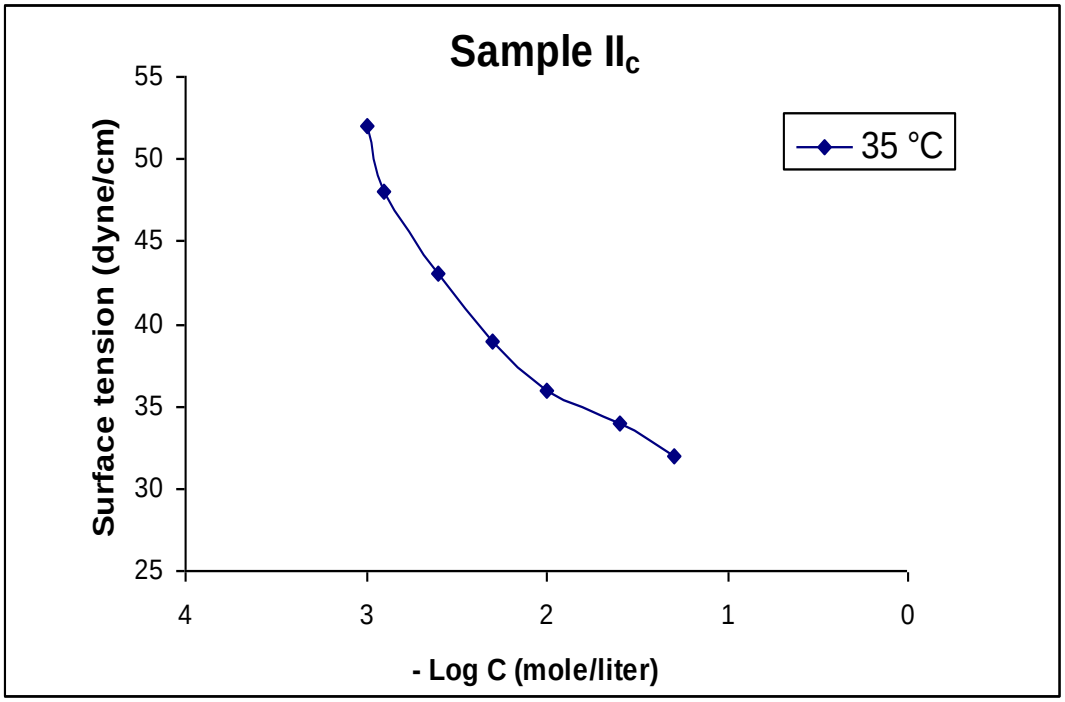

Fig. (28): Surface tension vs. – Log Concentration of sample (II_c) at (35 ºC).

Table (4): Surface tension at different temperatures and different concentrations of complex (M).

- log C	1.3	1.6	2	2.3	2.6	2.9	3
25 °C	33	34	35	37	41	47	53
35 °C	29	31	32	34	37	43	46
45 °C	28	30	31	33	36	38	39

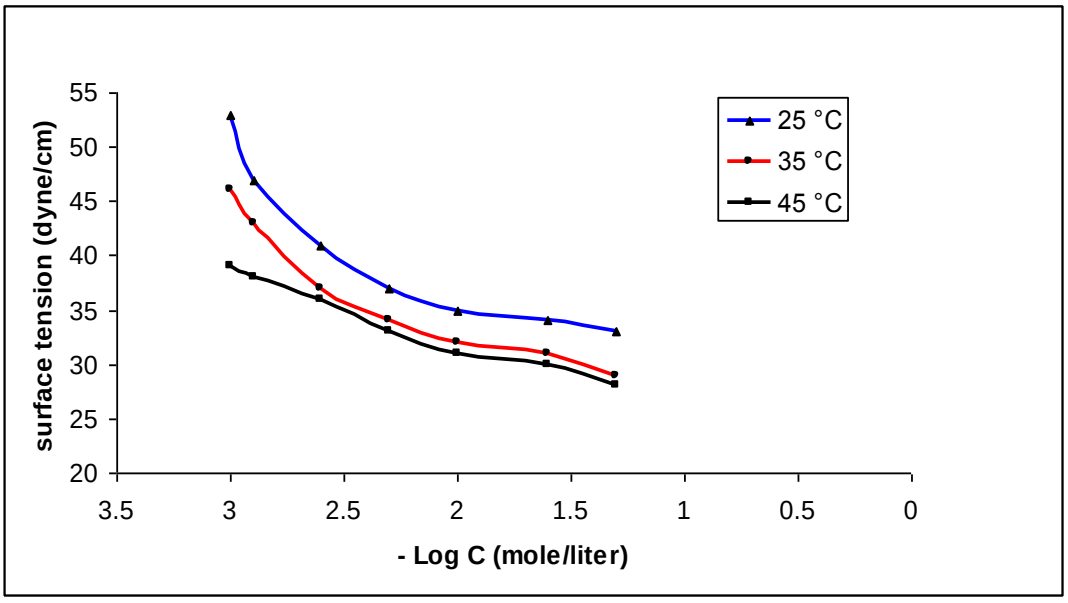

Fig. (29): Surface tension vs. – Log Concentration of complex (M) at different temperatures (25, 35, 45 ^{o}C).

Table (5): Surface tension at different temperatures and different concentrations of complex (N).

- Log C	1.3	1.6	2	2.3	2.6	2.9	3
25 °C	28	31	34	35	40	48	53
35 °C	27	30	33	34	39	43	47
45 °C	25	29	32	33	36.5	41	44

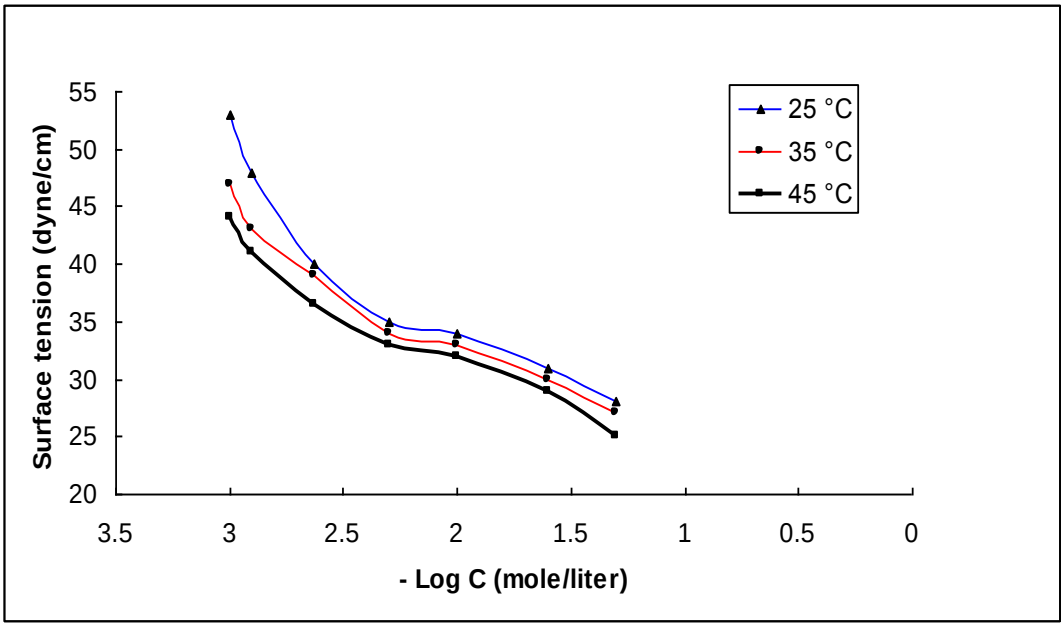

Fig. (30): Surface tension vs. – Log Concentration of complex (N) at different temperatures (25, 35, 45 ^{o}C).

Table (6): Surface tension at different temperatures and different concentrations of complex (X).

- Log C	1.3	1.6	2	2.3	2.6	2.9	3
25 °C	32	34	37	40	44	49	54
35 °C	31	33	35	37	39	46	49
45 °C	30	32	33	35	37	44	47

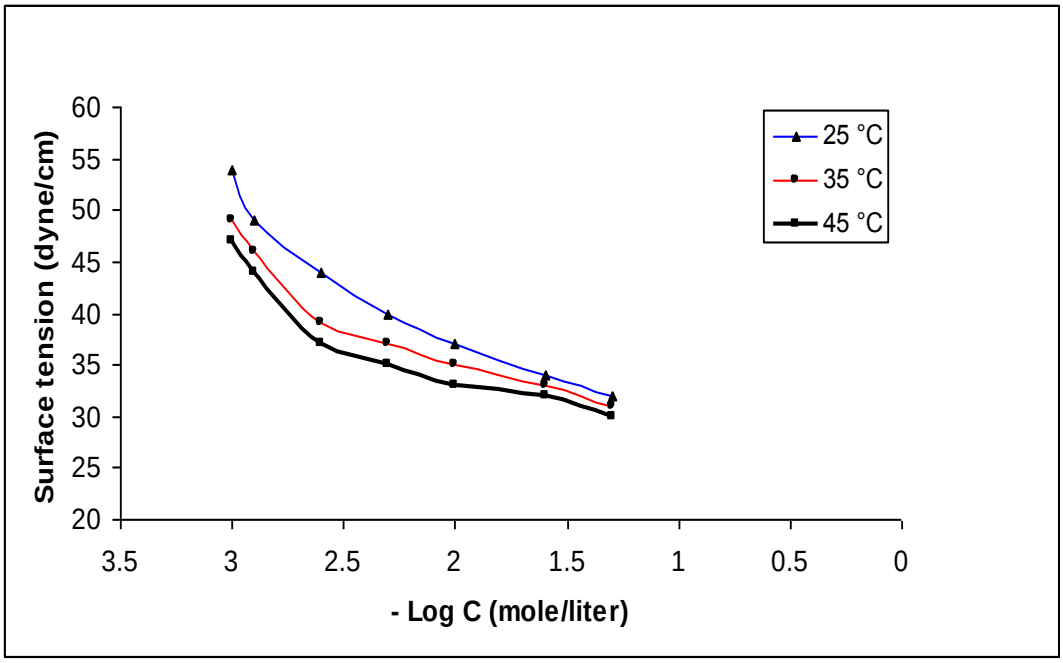

Fig. (31): Surface tension vs. – Log Concentration of complex (X) at different temperatures (25, 35, 45 ^{o}C).

Table (7): Surface tension at different temperatures and different concentrations of complex (Y).

- Log C	1.3	1.6	2	2.3	2.6	2.9	3
25 °C	31	33	35	37	42	47	55
35 °C	29	30	32	34	36	41	47
45 °C	28	29	31	32	34	38	41

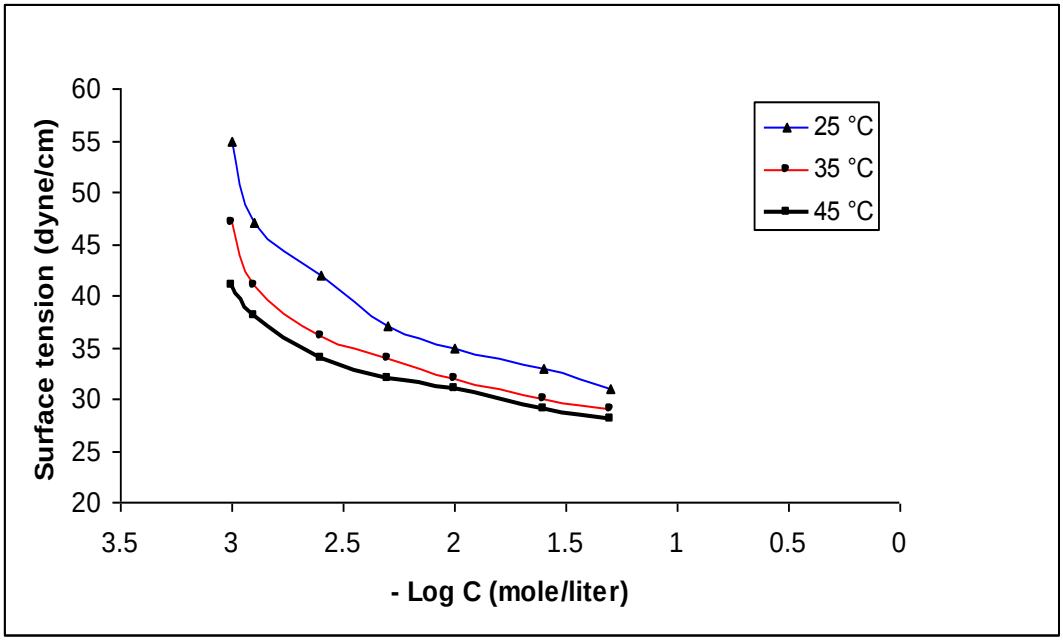

Fig. (32): Surface tension vs. – Log Concentration of complex (Y) at different temperatures (25, 35, 45 ^{o}C).

Table (8): Surface tension at different temperatures and different concentrations of complex (Z).

- Log C	1.3	1.6	2	2.3	2.6	2.9	3
25 °C	32	34	36	38	43	49	55
35 °C	29	31	34	37	42	47	50
45 °C	28	30	32	34	38	42	44

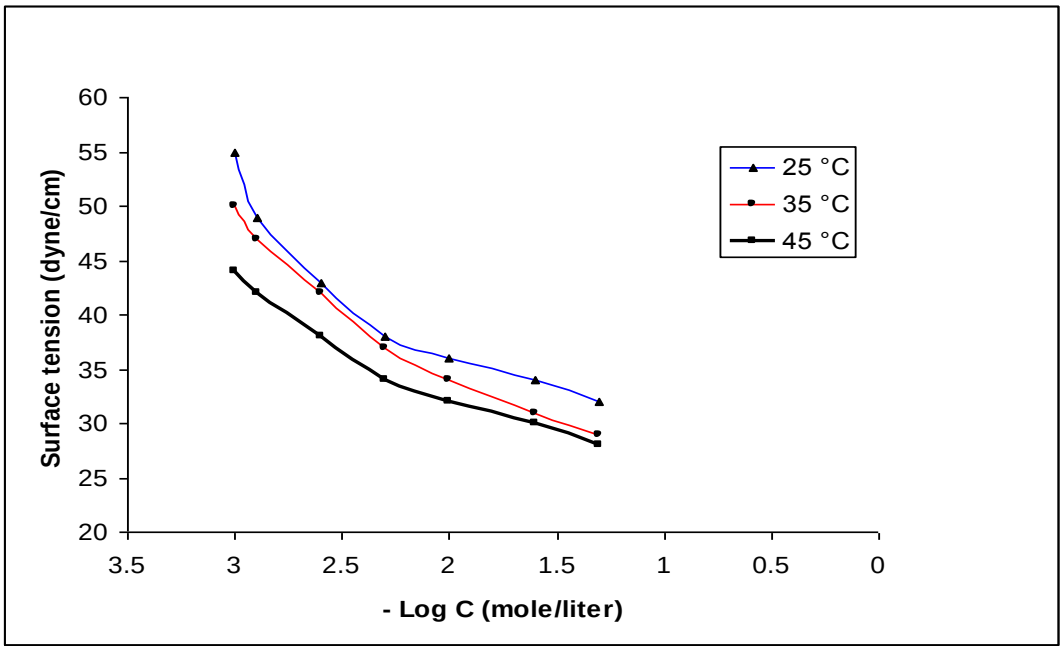

Fig. (33): Surface tension vs. – Log Concentration of complex (Z) at different temperatures (25, 35, 45 ^{o}C).

Table (9): Surface tension at different temperatures and different concentrations of complex (A).

- Log C	1.3	1.6	2	2.3	2.6	2.9	3
25 °C	37	39	43	47	48	53	56
35 °C	35	36	37	38	39	41	42
45 °C	34	35	36	37	38	40	41

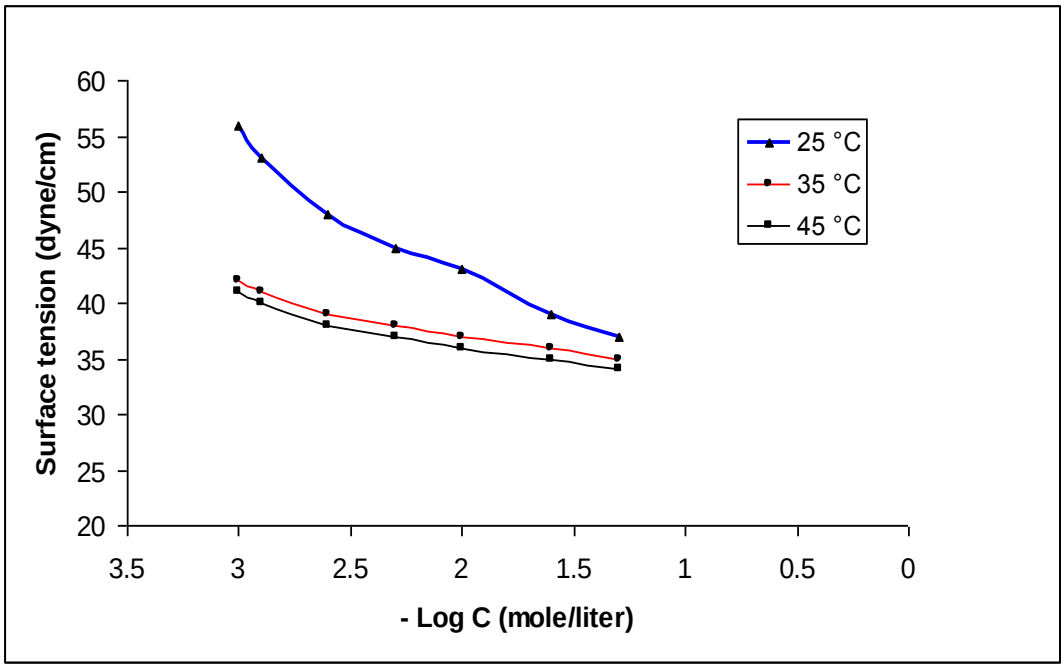

Fig. (34): Surface tension vs. – Log Concentration of complex (A) at different temperatures (25, 35, 45 ^{o}C).

Table (10): Surface tension at different temperatures and different concentrations of complex (B).

- Log C	1.3	1.6	2	2.3	2.6	2.9	3
25 °C	34	37	42	45	48	52	56
35 °C	33	35	39	41	43	46	47
45 °C	32	34	37	39	41	44	46

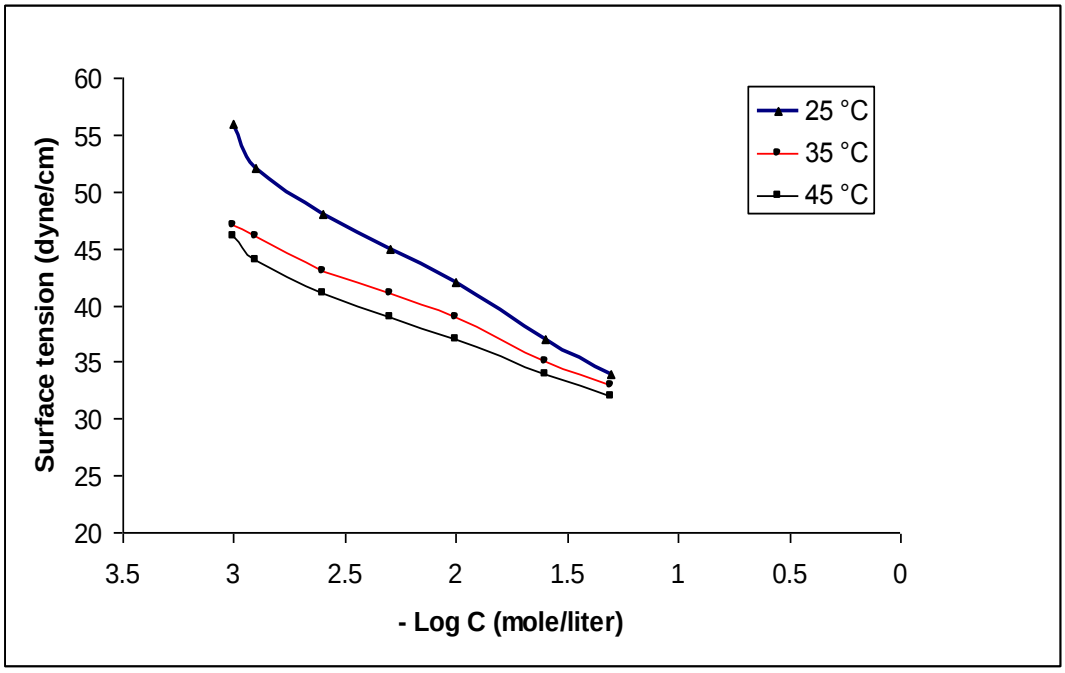

Fig. (35): Surface tension vs. – Log Concentration of complex (B) at different temperatures (25, 35, 45 ^{o}C).

2.3.3. Critical micelle concentration (CMC):

The critical micelle concentration is defined as the concentration of the surfactant at which no further decrease in the surface tension could be obtained upon addition of any further amounts of surfactant in the solution.

There is equilibrium between the singly adsorbed surfactant molecules at the interface and the micellized surfactant molecules. That equilibrium occurred at the concentration of complete surface saturation (CMC).

The micelle formation is the most vital point of view in the surfactant fundamental because it is the most effective geometric arrangement of the molecules at that desired concentration.

The surfactant molecules when dispersed in the water tend to be adsorbed at the interface, leading to decrease in the surface tension of the surfactant solutions. Further increase in the concentration is followed by gradual reduction of the surface tension until the surface of the solution becomes completely occupied by the surfactant molecules, after that the excess molecules tend to self aggregate in the bulk of the solution to form micelles.

Micelle formation or micellization is an important phenomenon because of a number of important interfacial properties such as detergency and solubilization.

From the intersection points in the surface tension profiles of the prepared complexes M, N, X, Y, Z, A and B, see Figs. (22-28), the values of the critical micelle concentrations (CMC) were determined.

Tables (11-13) list the critical micelle concentrations (CMC) of the prepared surfactants given from their surface tension at different temperatures 25, 35 and 45 °C.

It is clear that CMC values of the prepared complexes ranged between 2.86 X 10^{-3} to 1.82 X 10^{-3} mole/liter at 25 °C and 2.39 X 10^{-3} to 1.25 X 10^{-3} mole/liter at 35 °C and 2.23 X 10^{-3} to 9 X 10^{-4} mole/liter at 45 °C.

It has shown in the tables (11-13) that CMC values decrease as the number of hydrophobic chains increase in the same compound.

Which indicate that as the number of hydrophobic chains increase as the surfactant tends to micellize at lower concentration. That can be referred to the high repulsion forces occurred between the surfactant molecules and the aqueous phase. Then, the molecules form aggregates in their solutions at which the polar groups are facing the water phase while the non polar portions located in the center of aggregates.

Also, the critical micelle concentration (CMC) values decrease as the temperature increase from 25 to 45 ^{o}C and this is because the surfactants become less soluble due to the dehydration of the hydrophobic chain as the temperature increases.

2.3.4. Effectiveness (π_{CMC}):

The effectiveness of surfactant solution (π_{CMC}) is defined as the difference between the surface tension of the pure water (γ_o) and the surface tension of the surfactant solution at the critical micelle concentration (γ_{CMC}) at constant temperature.

$$\pi_{CMC} = \gamma_o - \gamma_{CMC} \quad \text{.....(1)}$$

Where (γ_o) is the surface tension for pure water at the appropriate temperature and (γ_{CMC}) is the surface tension at (CMC) of the substance.

Above the critical micelle concentration (CMC) the surface tension (γ) does not change much with the concentration; accordingly, (γ_{CMC}) used to calculate the values of the surface pressure (effectiveness).

The effectiveness values are considered a good variable in comparison between different surfactants in the same series. The most effective one (in one series of homologous) is that capable to decrease the surface tension at the critical micelle concentration to lower values at constant temperature.

Tables (11-13) list the effectiveness (π_{CMC}) of the prepared surfactants at different temperatures 25, 35 and 45 °C.

According to the results of the effectiveness, complex (Y) was found the most effective one at 25 °C, it gives 38.4 dyne/cm; it achieved the maximum reduction of surface tension at (CMC). While complexes (M and Y) were very close in their effectiveness and achieved the most effective ones at 35 °C, they give 41.62 and 41.17dyne/cm

respectively, complex (M) achieved the most effective one at 45 °C, it gives 42.4 dyne/cm.

Increasing the number of hydrophobic chains in the same compound like complexes (X, Y, Z, A and B) or the presence of two ligands coordinated to the metal ion like (M and N) complexes increase the interaction with the water phase and hence decrease the surface tension and increase the effectiveness according to equation (1). Also, by increasing the temperature the effectiveness increase for the same compound because the surfactant becomes less soluble due to the dehydration of the hydrophobic chain as the temperature increases, so the surface tension decrease.

2.3.5. Efficiency (Pc_{20}):

Efficiency (Pc_{20}) is determined by the concentration (mole/liter) of the surfactant solution which capable to reduce the surface tension of their solution by 20 dyne/cm at a certain temperature.

Therefore, the most effective surfactant is the one that gives a surface pressure of 52 dyne/cm at the lowest concentration.

The efficiency is an important parameter concern with the comparison between different homologues of surfactants. The efficiency values of the synthesized surfactants at different temperatures are shown in tables (11-13).

The efficiency mainly decreases with increasing the number of hydrophobic chains in the same compound or the presence of two ligands according to the metal ion. In addition, it decreases with increasing the temperature because the surfactant becomes less soluble

due to the dehydration of the hydrophobic chain as the temperature increases, so the surface tension decreases.

2.3.6. Maximum surface excess (Γ_{max}):

The number of surfactant molecules at the air-water interface can be calculated from surface tension values for the prepared surfactants (M, N, X, Y, Z, A and B) below the critical micelle concentration at 25, 35 and 45 °C according to Gibb's equation:

$$\Gamma_{max} = - 1 / 2.303\ RT \quad (\delta \gamma \ / \delta \log C)_T \ \ldots\ldots\ldots\ldots (2)$$

Where:

Γ_{max}	maximum surface excess in mole/cm^2
R	universal gas constant 8.31 x 10^7 ergs mole^{-1} K^{-1}
T	absolute temperature, K
$\delta \gamma$	surface pressure in dyne/cm
C	surfactant concentration

$(\delta\gamma/ \delta \log C)_T$ is the slope of plot surface tension vs. – log concentration curves below CMC at constant temperature.

The results were listed in tables (11-13).

A substance which lowers the surface energy is thus present in excess at or near the surface, i.e., when the surface tension decreases with increasing the activity of surfactants, (Γ_{max}) is positive.

Migration of surfactant molecules to the boundary surfaces between phases either air-liquid, solid-liquid or liquid-liquid phases to form adsorbed layer is one of the most objective application of surfactants as a vital branch of chemistry in several applications.

The maximum surface excess increases by increasing the number of hydrophobic chains in the same compound or by the presence of two ligands according to the metal ion due to increase the interaction with the water phase so the surfactant molecules are directed to the interface which decreases the surface energy of the solution.

2.3.7. Minimum surface area (A_{min}):

The minimum surface area is defined as the area occupied by each surfactant molecule at the air-water interface at the equilibrium of the solution, the average area occupied by each molecule adsorbed on the interface is given by:

$$A_{min} = 10^{16} / \Gamma_{max} N \text{ .....(3)}$$

Where:

Γ_{max} maximum surface excess in mole / cm^2

N Avogadro's number 6.023×10^{23}

The minimum surface area as a correspondence variable for the maximum surface excess depends on many factors included in the molecular structure, which are:

i. Ionized group.
ii. Polar part.
iii. Nonpolar part.
iv. Temperature.

The presence of more than one ionizable group within the surfactant molecule, e.g. diquaternary molecules increase the area occupied by the molecules at the interface.

This is due to increase the attachment points of each molecule at the interface. In monoquaternary surfactant molecules, the minimum surface area was found smaller than those of the diquaternary homologue with the hydrophobic structure. Polar groups also increase the minimum surface area in the same manner.

Values of the minimum surface area (A_{min}) per molecules at the aqueous air/water interface for the prepared complexes (M, N, X, Y, Z, A, and B) at different temperatures 25, 35 and 45 °C are presented in tables (11-13).

The minimum surface area (A_{min}) decreases with increasing the number of hydrophobic chains in the synthesized surfactant molecules due to the higher accumulation of theses molecules at the interface and hence the area available for each molecule being too small.

Table (11): Surface properties of the synthesized metallocationic surfactants at 25 °C.

Surfactant	CMC X 10^{-3}, mole/liter	π_{CMC}, dyne/cm	Pc_{20} X 10^{-3}, mole/liter	Γ_{max} X 10^{-10}, mole/cm^2	A_{min}, nm^2
M	2.37	36.35	1.0	1.352	1.228
N	2.86	38.15	1.0	1.617	1.027
X	2.71	36.23	1.12	1.296	1.281
Y	2.48	38.4	1.1	1.188	1.397
Z	2.4	36.17	1.02	1.336	1.243
A	1.87	26.77	1.2	0.842	1.972
B	1.82	27.66	1.12	0.732	2.269

Table (12): Surface properties of the synthesized metallocationic surfactants at 35 °C.

Surfactant	CMC X 10^{-3}, mole/liter	π_{CMC}, dyne/cm	Pc_{20} X 10^{-4}, mole/liter	Γ_{max} X 10^{-10}, mole/cm^2	A_{min}, nm^2
M	2.1	41.62	4.75	1.419	1.170
N	2.38	39.94	4.05	1.297	1.280
X	2.39	38.16	4.17	0.968	1.716
Y	2.05	41.17	5.48	1.250	1.328
Z	2.19	39.2	8.22	0.941	1.764
A	1.32	35.93	0.1	0.558	2.975
B	1.25	32	0.1	0.424	3.919

Table (13): Surface properties of the synthesized metallocationic surfactants at 45 °C.

Surfactant	**CMC X 10^{-3}, mole/liter**	**π_{CMC}, dyne/cm**	**Pc_{20} X 10^{-4}, mole/liter**	**Γ_{max} X 10^{-10}, mol/cm^2**	**A_{min}, nm^2**
M	1.74	42.4	0.656	1.600	1.037
N	2.1	40.97	1.76	1.287	1.290
X	2.23	39.88	1 .0	1.060	1.567
Y	1.78	41.7	0.26	1.256	1.322
Z	1.7	41	2.8	1.184	1.402
A	0.9	37	0.1	0.492	3.372
B	1.08	34.73	0.1	0.410	4.046

2.3.8. Thermodynamic parameters:

Adsorption and micellization processes of surfactant molecules are considered as phase transformation either from single state molecule in the solution into adsorbed molecules at the interface (adsorption) or into the well aggregated molecules in the form of micelles (micellization).

The thermodynamic parameters of adsorption and micellization of the synthesized cationic surfactants were calculated according to Gibb's adsorption equations as follows:

$$\Delta G^{O}_{mic} = RT \ln (CMC)$$

$$\Delta G^{O}_{ads} = \Delta G^{O}_{mic} - 6.023 \times 10^{-1} \times \pi_{CMC} \times A_{min}$$

$$\Delta S_{mic} = - d (\Delta G^{O}_{mic}) / \Delta T$$

$$\Delta S_{ads} = - d (\Delta G^{O}_{ads}) / \Delta T$$

$$\Delta H_{mic} = \Delta G^{O}_{mic} + T \Delta S_{mic}$$

$$\Delta H_{ads} = \Delta G^{O}_{ads} + T \Delta S_{ads}$$

ΔG^{O}_{mic}, ΔG^{O}_{ads}, ΔS_{mic}, ΔS_{ads}, ΔH_{mic} and ΔH_{ads} for the prepared metallosurfactants were calculated at different temperatures 25, 35 and 45 °C according to Gibb's equations of thermodynamics and their values are listed in tables (14-19).

Negative values of standard free energies of both micellization ΔG^{O}_{mic} and adsorption ΔG^{O}_{ads} for the prepared surfactants indicate that the micellization and adsorption are spontaneous processes.

The spontaneous process is contributed to the repulsion forces between the different hydrophobic moieties and the polar solvent.

Hence, as the number of hydrophobic parts increase as the tendency of theses molecules towards adsorption increase which result increase of the negativity values of ΔG^{O}_{ads}

However, the high negativity values of ΔG^{O}_{ads} showed that the process of adsorption is the most predominant process.

Furthermore, the negativity of the two process indicate that these two process are occurred in the same time with some prefer ability to the adsorption process. Obviously, the prepared cationic surfactants prefer adsorption at air/water interfaces due to high interactions between the hydrophobic chains and the polar medium.

Table (14): Thermodynamic parameters of micellization of the synthesized metallosurfactants at 25 °C.

Surfactant	ΔG^{O}_{mic}, KJ/mole	ΔS_{mic}, KJ/mole.K	ΔH_{mic}, KJ/mole
M	-14.982	-0.081	-39.196
N	-14.516	-0.096	-43.084
X	-14.650	-0.081	-38.923
Y	-14.870	-0.099	-44.302
Z	-14.951	-0.074	-36.898
A	-15.569	-0.142	-57.765
B	-15.637	-0.149	-59.979

Table (15): Thermodynamic parameters of adsorption of the synthesized metallosurfactants at 25 °C.

Surfactant	ΔG^{O}_{ads}, KJ/mole	ΔS_{ads}, KJ/mole.K	ΔH_{ads}, KJ/mole
M	-41.867	-0.105	-73.298
N	-38.092	-0.168	-88.159
X	-42.603	-0.196	-101.110
Y	-47.180	-0.105	-78.431
Z	-42.030	-0.219	-107.425
A	-47.365	-0.467	-186.714
B	-53.421	-0.526	-210.333

Table (16): Thermodynamic parameters of micellization of the synthesized metallosurfactants at 35 °C.

Surfactant	ΔG^{O}_{mic}, KJ/mole	ΔS_{mic}, KJ/mole.K	ΔH_{mic}, KJ/mole
M	-15.794	-0.081	-40.820
N	-15.474	-0.096	-44.999
X	-15.463	-0.081	-40.551
Y	-15.856	-0.099	-46.275
Z	-15.687	-0.074	-38.370
A	-16.984	-0.142	-60.594
B	-17.123	-0.149	-62.953

Table (17): Thermodynamic parameters of adsorption of the synthesized metallosurfactants at 35 °C.

Surfactant	ΔG^{o}_{ads}, KJ/mole	ΔS_{ads}, KJ/mole.K	ΔH_{ads}, KJ/mole
M	-45.099	-0.105	-77.583
N	-46.265	-0.168	-98.012
X	-54.903	-0.196	-115.372
Y	-48.786	-0.105	-81.085
Z	-57.335	-0.219	-124.923
A	-81.365	-0.467	-225.387
B	-92.657	-0.526	-254.831

Table (18): Thermodynamic parameters of micellization of the synthesized metallosurfactants at 45 °C.

Surfactant	**ΔG^{O}_{mic}, KJ/mole**	**ΔS_{mic}, KJ/mole.K**	**ΔH_{mic}, KJ/mole**
M	-16.804	-0.101	-48.942
N	-16.307	-0.083	-42.813
X	-16.148	-0.069	-37.945
Y	-16.744	-0.089	-45.000
Z	-16.866	-0.118	-54.381
A	-18.548	-0.156	-68.314
B	-18.066	-0.094	-48.040

Table (19): Thermodynamic parameters of adsorption of the synthesized metallosurfactants at 45 °C.

Surfactant	ΔG^{o}_{ads}, KJ/mole	ΔS_{ads}, KJ/mole.K	ΔH_{ads}, KJ/mole
M	-43.287	-0.073	-66.420
N	-48.115	-0.094	-77.866
X	-53.763	-0.050	-69.737
Y	-49.947	-0.092	-79.063
Z	-51.487	-0.048	-66.633
A	-93.693	-0.264	-177.698
B	-102.699	-0.185	-161.630

2.4. Biological activity of the metallosurfactant complexes:

The cell membrane of microorganisms is composed of several lipids and protein layers arranged together in specific arrangement called the bilayer (or multilayer lipoprotein structure). The presence of lipids as a building unit in the cell membranes acquires them their hydrophobic character. The selective permeability of such lipoprotein membrane represents the main parameter controlling the biological reactions in the cell. Hence, any factor influencing the permeability causes a great damage to the microorganism leading to its death.

The antimicrobial activity of the prepared metallocationic surfactants (M, N, X, Y, Z, A and B) was measured individually against a wide range of microorganisms previously isolated in Biotechnology Lab. in Egyptian Petroleum Research Institute (EPRI) from different oil polluted environments using dose equal to 5 mg/l by the diffusion agar technique.

The microorganisms includes Gram-positive bacteria (Staphylococcus gallinarum NK1, Bacillus maroccanus I.1.1.3 and Brevibacterium casei I.2.1.7), Gram-negative bacteria (Pseudomonas synxantha I.1.1.1), Yeast (Candida parapsilosis NSh45) and Fungi (Aspergillus terreus I.1.3.1).

The data of biological activity of the synthesized metallocationic surfactants (M, N, X, Y, Z, A and B) listed in table (20).

Gram-positive bacteria, Gram negative bacteria, Yeast and Fungi were affected extremely by all the synthesized metallocationic surfactants except complex (B) while Gram-positive bacteria called

Brevibacterium casei I.2.1.7, Gram-negative bacteria, Yeast and Fungi not affected by complex (A).

The synthesized metallocationic surfactants (M, N, X, Y, Z and A) showed high biological activity due to:

i. The ionization of the molecules under investigation in the aqueous media produces different ions; the produced metal cations are attracted to the negatively charged cell membrane and neutralize its charge. Hence, its selective permeability is distorted.
ii. The halogen ions penetrate into the cytoplasm of the cell, which inactivate the essential metabolic compounds such as proteins and enzymes. The inactivation action proceeded via oxidation of these proteins resulting in the bacterial cells die.

Table (20): Microbial inhibition zone of tested complexes in millimeters.

Microorganism / Compounds ID	NK1	I.1.1.3	I.2.1.7	I.1.1.1	NSh45	I.1.3.1
M	26	38	23	22	22	18
N	20	25	20	20	16	14
X	24	21	15	20	18	14
Y	20	24	16	18	16	16
Z	18	20	18	18	17	14
A	16	11	Nil	Nil	Nil	Nil
B	Nil	Nil	Nil	Nil	Nil	Nil

2.5. Antimicrobial activity of the prepared surfactants against sulfate reducing bacteria (SRB):

Generally, biocides exert their bacteriostatic effect on sensitive organisms by:

i. Inhibit the permeability of the cell wall.
ii. Injure the cytoplasmic membrane.
iii. Inhibit the protein biosynthesis.
iv. Inhibit the nucleic acid synthesis.

The increase in microorganisms in the system (petroleum tanks for example) has led to a variety of problems. Among these microorganisms a bacteria found in biofilm called sulfate reducing bacteria (SRB), anaerobic microorganisms often found under accumulated deposits where the oxygen tension is low. These organisms are capable of reducing sulfate to sulfide, an acidic by-product responsible for many corrosion and odor problems. Sulfide can also react with certain biocide, rendering them ineffective against other microorganisms present in the system.

Control of microorganisms, especially (SRB) is important to success of any biocide treatment program.

The results of antimicrobial activity of the synthesized biocides (X, Y and Z) against sulfate reducing bacteria (SRB) were determined by dilution method and listed in table (21).

The results indicate that the synthesized metallocationic surfactants have antimicrobial activity against the tested organisms (SRB) and

their activities depend on their chemical structure mainly the number of the hydrophobic chains and their length and the kind of metal.

The action mode of such cationic biocides on the bacterial strain is explained as an electrostatic interaction and physical disruption. The electrostatic interaction occurs between the oppositely charged centers on the cellular membrane and the positively charged head group of the biocide molecules. While, physical disruption is result from the penetration of the hydrophobic chains into the cellular membrane due to the similarity of the chemical nature.

The interaction between the biocide molecules and cellular membrane causes a strong damage of the selective permeability of these membranes which disturb the metabolic pathway within the cytoplasm.

Table (21): Antimicrobial activity of some synthesized surfactants against SRB by dilution method.

Dose, ppm / Days	Bacteria Count (SRB)								
	Sample X			Sample Y			Sample Z		
	800	1000	1200	800	1000	1200	800	1000	1200
1	0.0	0.0	0.0	0.0	0.0	0.0	0.0	0.0	0.0
2	10^2	0.0	0.0	0.0	0.0	0.0	0.0	0.0	0.0
3	10^2	0.0	0.0	10^3	10^3	10^3	10^3	10^2	10
4	10^2	10^2	10	10^3	10^3	10^3	10^3	10^3	10^2
5	10^2	10^2	10	10^3	10^3	10^3	10^3	10^3	10^3
6	10^3	10^3	10^3	10^3	10^3	10^3	10^3	10^3	10^3